Article

Current Biology

Ancient genomes reveal structural shifts after the arrival of Steppe-related ancestry in the Italian Peninsula

Highlights

- 22 genomes from Northeastern and Central Italy dated between 3200 and 1500 BCE
- Arrival of Steppe-related ancestry in the central Italian Peninsula by 1600 BCE
- Close patrilineal kinship patterns within commingled Chalcolithic cave burials
- Roman Imperial period had a stronger effect on phenotype shifts than the Bronze Age

Authors

Tina Saupe, Francesco Montinaro, Cinzia Scaggion, ..., Cristian Capelli, Luca Pagani, Christiana L. Scheib

Correspondence

tina.saupe@ut.ee (T.S.), cls83@ut.ee (C.L.S.)

In brief

Using ancient DNA sequences from the Italian Peninsula, Saupe et al. explore the genetic history of the Italian Peninsula through the Chalcolithic/Bronze Age transition. The time transect shows Steppe-related ancestry arrived in Central Italy by 1600 BCE and possibly precipitated shifts in kinship patterns, but not phenotypes.

Saupe et al., 2021, Current Biology *31*, 2576–2591
June 21, 2021
https://doi.org/10.1016/j.cub.2021.04.022

CellPress

CellPress
OPEN ACCESS

Current Biology

Article

Ancient genomes reveal structural shifts after the arrival of Steppe-related ancestry in the Italian Peninsula

Tina Saupe,[1,26,27,*] Francesco Montinaro,[1,2,26] Cinzia Scaggion,[3] Nicola Carrara,[4] Toomas Kivisild,[1,5] Eugenia D'Atanasio,[6] Ruoyun Hui,[7] Anu Solnik,[8] Ophélie Lebrasseur,[9,10] Greger Larson,[12] Luca Alessandri,[11] Ilenia Arienzo,[12] Flavio De Angelis,[13] Mario Federico Rolfo,[14] Robin Skeates,[15] Letizia Silvestri,[14] Jessica Beckett,[16] Sahra Talamo,[17,18] Andrea Dolfini,[19] Monica Miari,[20] Mait Metspalu,[1] Stefano Benazzi,[21] Cristian Capelli,[22,23,26] Luca Pagani,[1,24,26] and Christiana L. Scheib[1,25,26,*]

[1]Estonian Biocentre, Institute of Genomics, University of Tartu, Riia 23B, Tartu 51010, Estonia
[2]Department of Biology-Genetics, University of Bari, Via E. Orabona, 4, Bari 70124, Italy
[3]Department of Geosciences, University of Padova, Via Gradenigo 6, Padova 35131, Italy
[4]Museum of Anthropology, University of Padova, Palazzo Cavalli, via Giotto 1, Padova 35121, Italy
[5]Department of Human Genetics, KU Leuven, Leuven, Herestraat 49 3000, Belgium
[6]Institute of Molecular Biology and Pathology, CNR, Piazzale Aldo Moro 5, Rome 00185, Italy
[7]McDonald Institute for Archaeological Research, University of Cambridge, Downing Street, Cambridge CB2 3ER, UK
[8]Core Facility, Institute of Genomics, University of Tartu, Riia 23B, Tartu 51010, Estonia
[9]Department of Archaeology, Classics and Egyptology, University of Liverpool, 12-14 Abercromby Square, Liverpool L69 7WZ, UK
[10]Palaeogenomics & Bio-Archaeology Research Network, School of Archaeology, University of Oxford, 1 South Parks Road, Oxford OX1 3TG, UK
[11]Groningen Institute of Archaeology, University of Groningen, Poststraat 6, Groningen 9712, the Netherlands
[12]Istituto Nazionale di Geofisica e Vulcanologia, Osservatorio Vesuviano, Via Diocleziano 328, Naples 80125, Italy
[13]Centre of Molecular Anthropology for Ancient DNA Studies, Department of Biology, University of Rome "Tor Vergata," Via della Ricerca Scientifica 1, Rome 00133, Italy
[14]Department of History, Culture and Society, University of Rome "Tor Vergata," Via Columbia 1, Rome 00133, Italy
[15]Department of Archaeology, Durham University, Lower Mountjoy, South Road, Durham DH1 3LE, UK
[16]Independent scholar, Cagliari, Italy
[17]Department of Chemistry "Giacomo Ciamician," University of Bologna, Via Selmi 2, Bologna 40126, Italy
[18]Department of Human Evolution, Max Planck Institute for Evolutionary Anthropology, Deutscher Platz 6, Leipzig 04103, Germany
[19]School of History, Classics and Archaeology, Newcastle University, Newcastle upon Tyne NE1 7RU, UK
[20]Superintendency of Archeology, Fine Arts and Landscape for the metropolitan city of Bologna and the provinces of Modena, Reggio Emilia and Ferrara, Comune di Bologna, Sede Via Belle Arti n. 52, Bologna 40126, Italy
[21]Department of Cultural Heritage, University of Bologna, Via degli Ariani, 1, Ravenna 40126, Italy
[22]Department of Zoology, University of Oxford, 11a Mansfield Road, Oxford OX1 3SZ, UK
[23]Dipartimento di Scienze Chimiche, della Vita e della Sostenibilità Ambientale, University of Parma, Parco Area delle Scienze 17/A, Parma 43124, Italy
[24]Department of Biology, University of Padova, Via U. Bassi, 58/B, Padova 35122, Italy
[25]St. John's College, University of Cambridge, St. John's Street, Cambridge CB2 1TP, UK
[26]These authors contributed equally
[27]Lead contact
*Correspondence: tina.saupe@ut.ee (T.S.), cls83@ut.ee (C.L.S.)
https://doi.org/10.1016/j.cub.2021.04.022

SUMMARY

Across Europe, the genetics of the Chalcolithic/Bronze Age transition is increasingly characterized in terms of an influx of Steppe-related ancestry. The effect of this major shift on the genetic structure of populations in the Italian Peninsula remains underexplored. Here, genome-wide shotgun data for 22 individuals from commingled cave and single burials in Northeastern and Central Italy dated between 3200 and 1500 BCE provide the first genomic characterization of Bronze Age individuals (n = 8; 0.001–1.2× coverage) from the central Italian Peninsula, filling a gap in the literature between 1950 and 1500 BCE. Our study confirms a diversity of ancestry components during the Chalcolithic and the arrival of Steppe-related ancestry in the central Italian Peninsula as early as 1600 BCE, with this ancestry component increasing through time. We detect close patrilineal kinship in the burial patterns of Chalcolithic commingled cave burials and a shift away from this in the Bronze Age (2200–900 BCE) along with lowered runs of homozygosity, which may reflect larger changes in population structure. Finally, we find no evidence that the arrival of Steppe-related ancestry in Central Italy directly led to changes in frequency of 115 phenotypes present in the dataset, rather that the post-Roman

Imperial period had a stronger influence, particularly on the frequency of variants associated with protection against Hansen's disease (leprosy). Our study provides a closer look at local dynamics of demography and phenotypic shifts as they occurred as part of a broader phenomenon of widespread admixture during the Chalcolithic/Bronze Age transition.

INTRODUCTION

The Italian Chalcolithic (or Copper Age [CA]; 3600–2200 BCE), the period between the Late Neolithic (N) (7000–3600 BCE) and the Bronze Age (BA) (2200–900 BCE), is characterized by the development of new tools from different metallic sources and was followed by major cultural transformations, including that of burial practice—from an emphasis on the collective to the individual and of personal, prestige grave goods.[1,2] Ancient DNA (aDNA) studies have highlighted the occurrence of major shifts in the genetic profiles of populations coinciding with material culture changes, such as from hunting-gathering to farming.[3–6] At the beginning of the transition from the Chalcolithic to the BA ~5,000 years ago, people from the Eurasian Steppe arrived in Europe, resulting in further admixing with local populations.[7–10] Although these events have been extensively studied in most of Europe[4,11,12] and a number of studies on ancient genomes from the Italian Peninsula, Sardinia, and Sicily have been recently published,[4,7,9,13–17] the demographic dynamics of the Chalcolithic/Early BA in the Italian Peninsula are still not well characterized. Though previous studies place the arrival of a Steppe-related ancestry component in Northern Italy[9] and in Sicily[16] after 2300 BCE, a chronological gap from 1900 to 900 BCE is present, and little is known about the spread of Steppe-related ancestry in Central Italy. In addition, the available data show an Iranian N-related component detected in Sardinia after 900 BCE,[16,17] although affinities to Caucasus hunter-gatherers (CHG) and Iran N farmers are present in Central Italian N individuals[13] and in Middle BA Sicily,[16] at a lower proportion than modern Italians.[11] However, although the BA CHG affinity in Sicily is supported by $f4$ statistics, the evidence for the N CHG influx is less robust. Furthermore, with a few exceptions,[18,19] previous surveys have focused primarily on describing ancestral relationships or inferring movement and mixtures of populations at the expense of questions focusing on the social dynamics associated with these events, e.g., evaluating the kinship structure in prehistoric society.

aDNA is proving a useful tool for helping to infer past social structures and reproductive behavior (reviewed in Racimo et al.[20]). In N Europe, several studies have detected a widespread cultural connection of patrilineal social organization[21,22] as well as for the BA transition with large-scale, sex-biased migrations,[8,23,24] local patterns of patrilocality and female exogamy,[18,25] and the influence of cultural diffusion versus migration.[9] Although the social implications of these changes are still debated,[26] cultural shifts can have an effect on adaptation (e.g., a change in technology leads to a change in diet, leading to selective pressure on metabolism genes). So far, the social structure(s) in Central Italy during the Chalcolithic/BA transition and whether shifts in cultural practices (kinship, patrilocality, and exogamy) correlate with the introduction of Steppe-related ancestry remains unexplored. This may be partially due to the fact that, although there exists a wide variety of burial practices in the Chalcolithic period in Italy, they are often characterized by collective depositions of commingled remains.[2] This has made the anthropological analysis of the burial populations and interpretations regarding kinship and social structure difficult; however, high-throughput aDNA sequencing allows for the genetic screening of large numbers of skeletal samples and reconstruction of individuals from disarticulated remains.

In addition to reshaping our understanding of the demographic history of the European continent, analyses of ancient genomes from Europe have recently called into question hypotheses regarding the time depth of selection on phenotypic traits in Europe. For example, aDNA has revealed that Mesolithic hunter-gatherers in Europe could have dark skin and blue eyes (a combination rarely seen today)[27–29] and that selection on skin pigmentation occurred in the last 5,000 years.[30,31] Other recent work has suggested that selection within genes related to fatty acid metabolism and starch digestion did not take place during the transition to agriculture but instead initiated closer to 2000 BCE following the introduction of Steppe-related ancestry into Europe,[31] with the ancestry component itself a possible driver. Another open question, that of the role of pathogens in shaping human genomes, is now starting to be explored using aDNA. One particular pathogen, Hansen's disease (leprosy), is first seen in paleopathological evidence in the Mediterranean dating to the BA[32] and is noted in Central and Northeast Italy by 300 BCE.[33] The disease may have been later spread by Roman military movements[34] and increased to high numbers in Europe in the Early Medieval Period, but declined by the 15th century CE, and the role of human genetic adaptation in this decline is unknown. There are a number of genetic loci that have been implicated in the manifestation and progression of the infection,[35–38] including one recently discovered using aDNA.[39]

Here, using an aDNA approach, we investigated the diversity of ancestry components prior to and through the Chalcolithic/BA transition in Northeastern and Central Italy and whether shifts in Steppe-related ancestry correlate with changes in inferred social structure and/or phenotypic traits.

RESULTS

We extracted DNA from 51 skeletal elements (teeth = 37, petrous bones = 10, and additional powder from petrous bones = 4) at the Ancient DNA Laboratory of the Institute of Genomics, University of Tartu in Estonia. The human remains are from one necropolis (Necropoli di Gattolino; hereafter, "Gattolino") and three cave sites located in Northeastern (Grottina dei Covoloni del Broion: "Broion") and Central Italy (Grotta La Sassa: "La Sassa" and Grotta Regina Margherita: "Regina Margherita"; Figures 1A and S1). After screening 47 libraries at a low depth (±20M reads per library), we identified and sequenced 20 libraries with more than 4% endogenous human DNA and mtDNA-based contamination estimates less than 1.44% (Data S1A and S1B). For the disarticulated

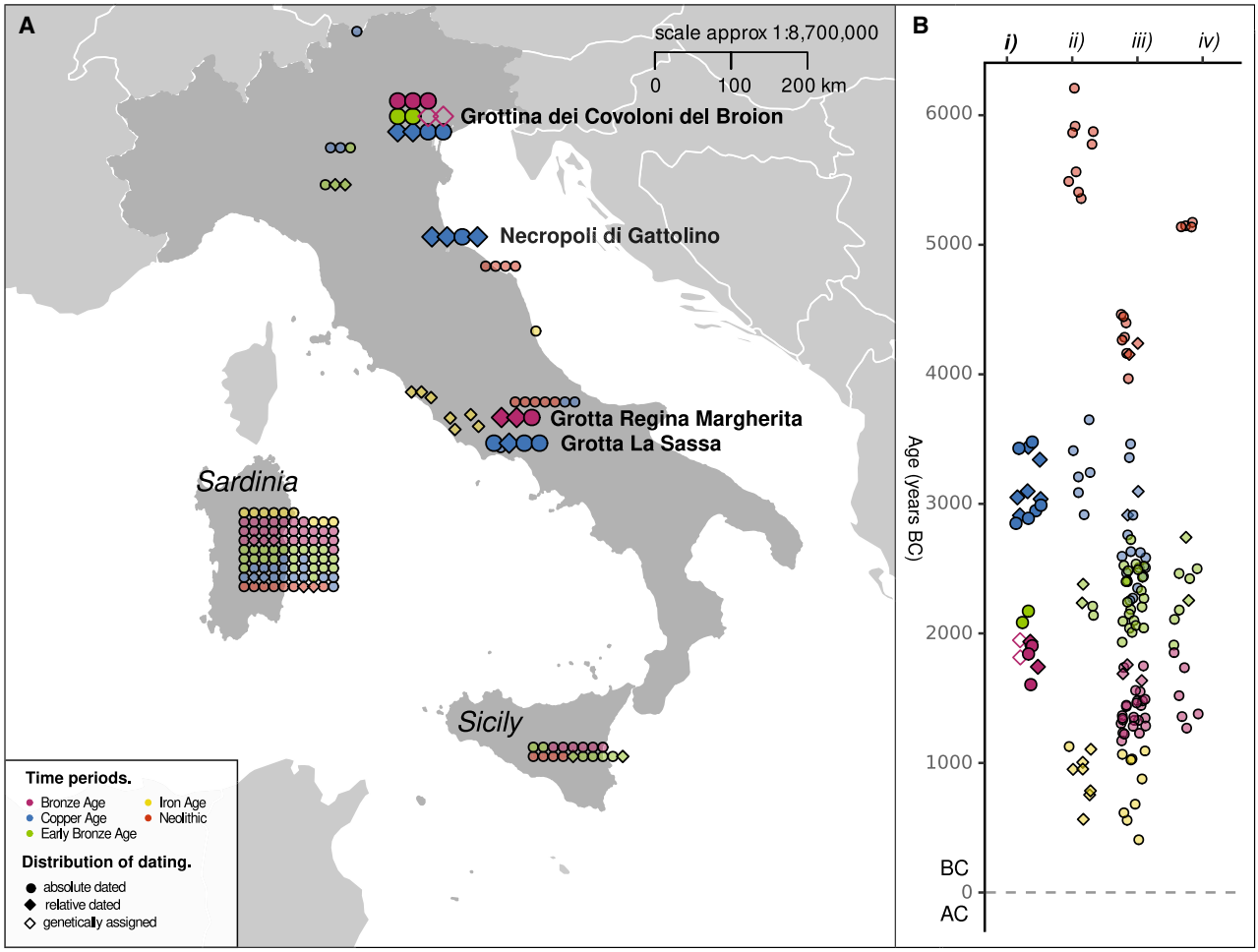

Figure 1. Geographical location of samples and relative or absolute dating

(A) Map of the geographical location of selected published (smaller, transparent) and newly generated samples from the Italian Peninsula, Sardinia, and Sicily included in this study. The titled locations are here newly reported. See also Table 1 and Data S1.

(B) Distribution of relative and absolute dating and genetic assignment from newly generated samples (i) and published (transparent; order: [ii] Italian Peninsula; [iii] Sardinia; and [iv] Sicily).

See also Data S1A–S1D.

remains in the cave sites, we calculated the pairwise mismatch rate of SNPs (P0) on pseudo-haploid data as implemented in READ[40] to identify genetically identical samples and attempt to calculate a minimum number of individuals (see STAR Methods and Data S1B for details).

The sequences of identical samples were merged together, leaving 22 unique individuals: eleven from Broion (Italy_Broion_CA = 4, Italy_Broion_EBA = 2, and Italy_Broion_BA = 5), four from Gattolino (Italy_Gattolino_CA), three from Regina Margherita (Italy_ReginaMargherita_BA), and four from La Sassa (Italy_LaSassa_CA). The final data are composed of individuals with endogenous DNA between 0.48% and 48.87%, average genomic coverage between 0.0016× and 1.24×, and estimated contamination rates of 0.00%–1.44% (mtDNA-based) and 0.45%–1.98% (X-chromosome-based in males only; Table 1; Data S1A and S1B).

In order to characterize the timing of genetic shifts related to the presence of ancestry from the Steppe and to assign individuals in commingled contexts within chronological space, we relied on two forms of temporal assignment: archaeological evidence (e.g., ceramic fragments, a significant amount of metallic tools found with the human remains, and geological layers; STAR Methods) and direct radiocarbon dating of 12 of the 22 individuals here sequenced (Figure 1B; Data S1C; STAR Methods). Of the ten undated samples, the age of BRC013 can be inferred as ± the average reproductive span of a woman (30 years) to a directly dated sample (BRC022) from the first-degree relatedness (likely brothers), although for the other nine (BRC007, BRC011, BRC024, LSC011A1, GCP002A1, GCP004A1, GLR001A1, GLR002A1, and GLR004), we assigned them to the most parsimonious group, considering both archaeological and genetic information.

Genetic structure of Italy from the N to the Iron Age

To compare Chalcolithic and BA individuals from Italy to other ancient and contemporary European populations, we performed

Table 1. Archaeological information, genome coverage, genetic sex, mtDNA, and Y chromosome haplogroups of the individuals of this study

Individual	Site	Date	Genome coverage	Gen. sex	mtDNA HG	Y chromosome HG	No. of SNPs
BRC001/023	Broion	4430 ± 40 BP; 3313–2934 cal BCE	0.172	XY	J2a1a1	G2a3-F1193-F2291	231,702
BRC002	Broion	failed C14 dating	0.143	XY	N1a1a1a1	R1b1-DF90	200,133
BRC003	Broion	3239 ± 31 BP[a]; 1532–1452 cal BCE	1.235	XY	U4a2f	R1b1'5-P312	920,226
BRC007/019	Broion	3272 ± 29 BP; 1608–1502 cal BCE	0.189	XX	K1a1b1	–	259,050
BRC010/018	Broion	3532 ± 35 BP; 1926–1775 cal BCE	0.360	XX	H+16291T	–	437,478
BRC011	Broion	not dated	0.0025	XY	T2c1+146T!	–	3,606
BRC013	Broion	failed C14 dating	0.052	XY	H5a1[b]	G2a3-F705	70,071
BRC015	Broion	not dated	0.0016	XY	T2c1e	–	2,145
BRC022	Broion	4489 ± 41 BP; 3334–3100 cal BCE	0.145	XY	H5a1[b]	G2a3-F1193	188,166
BRC024	Broion	not dated	0.0144	XY	HV0a	R1	19,590
BRC030	Broion	3502 ± 41 BP; 1886–1751 cal BCE	0.110	XX	K1a4a1e	–	145,106
GCP002	Regina Margherita	failed C14 dating	0.138	XY	U5b2b5	G2	181,152
GCP003	Regina Margherita	3277 ± 29 BP; 1608–1504 cal BCE	0.138	XX	H3am	–	180,991
GCP004	Regina Margherita	not dated	0.0052	XX	U5b2b3	–	7,278
GLR001	Gattolino	not dated	0.214	XX	K2b1b	–	262,814
GLR002	Gattolino	not dated	0.129	XY	J1c3e1	I2d-L623/M223	163,883
GLR003	Gattolino	4829–4627 BP; 2874–2704 cal BCE	0.008	XX	H10d	–	10,863
GLR004	Gattolino	not dated	0.122	XY	H3am	I2b-M26	157,772
LSC002/004	La Sassa	4091 ± 29 BP: 2840–2575 cal BCE	1.014	XY	H1bv1[b]	J2a7-Z2397	903,958
LSC005/013	La Sassa	4097 ± 39 BP; 2847–2575 cal BCE	0.1323	XX	H1e5a	–	176,120
LSC007	La Sassa	not dated	0.0029	XY	H1bv1[b]	–	4,033
LSC011	La Sassa	4073 ± 37 BP; 2837–2498 cal BCE	0.063	XY	J1c1	J2a-M410 (J2a7-Z2397)	83,596

Dates in BP are raw radiocarbon dates; calibrated dates are the 68.3% probability and were calibrated using IntCal20[41] and either CALIBREV8.2[42] or OxCal 4.4[43] (GLR003). See also Data S1. Gen., genetic; HG, haplogroup.

[a]Sample failed C14 dating, but a genetically identical sample was able to be dated

[b]Indicates identical haplotype

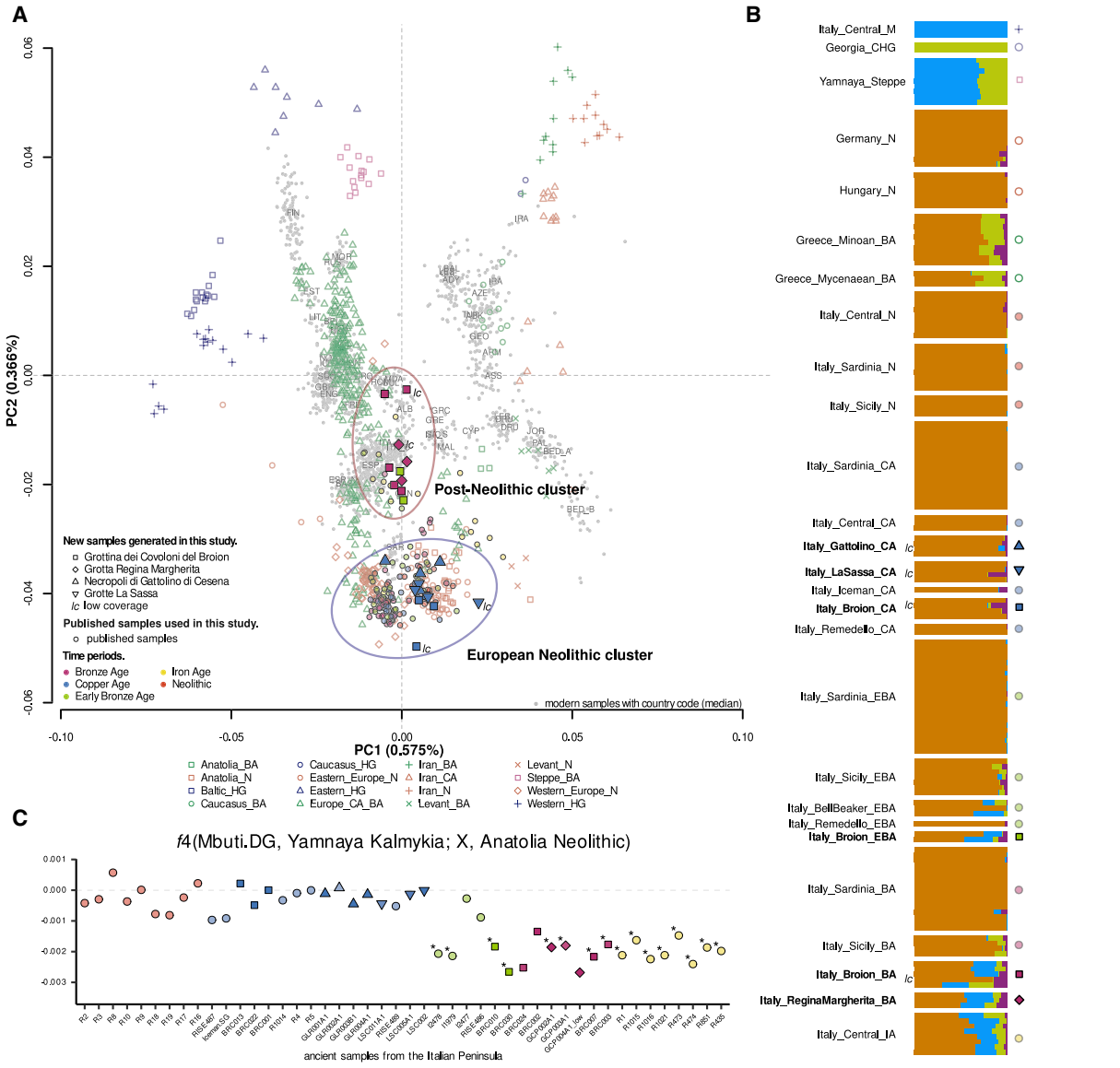

Figure 2. Overview of genetic structure

(A) Principal component analysis (PCA) of newly generated individuals with previously published data projected onto the variation from present-day populations (Data S1D).

(B) DyStruct analysis of newly reported ancient individuals (bold) numerically ordered at K = 4 together with a subset of key ancient Eurasian populations spanning from Neolithic to Iron Age. The icons on the right of the graph indicate the symbols of the population as shown on the PCA in (A). Samples with *lc* indicate low coverage samples generated in this study. See also Figures S2–S4A.

(C) Analysis of the Steppe-related ancestry components in selected published (transparent) and newly generated ancient samples (X) from the Italian Peninsula using $f4$ statistics in form $f4$(Mbuti.DG, Yamnaya Kalmykia; X, Anatolia Neolithic) (samples with * have a Z score less than or equal to -3). Tests with less than 5,000 SNPs were not included.

See also Data S2B and Figure S4B.

principal-component analysis (PCA), projecting ancient samples onto the genetic variation of 1,471 present-day individuals from Eurasia (Figures 2A and S4A).[44,45] Our newly generated samples scatter into two main clusters: European N (EN) (blue circle) encompassing all the Chalcolithic samples (Italy_LaSassa_CA, Italy_Gattolino_CA, and Italy_Broion_CA) and post-Neolithic (PN) (red circle), including Early Bronze and BA samples from Grotta Regina Margherita and Broion. Interestingly, most of the N, Chalcolithic, and BA Italian samples available from the literature fall within the EN cluster, although PN is mostly featuring Iron Age (IA) samples together with a few published BA individuals. This can be reconciled by the fact that most of the Italian BA samples available to date come from Sardinia and Sicily, two Mediterranean islands for which a reduced Steppe-related ancestry component has already been reported.[6,11,16,17,46] This is confirmed by DyStruct analysis (Figures 2B and S2), which

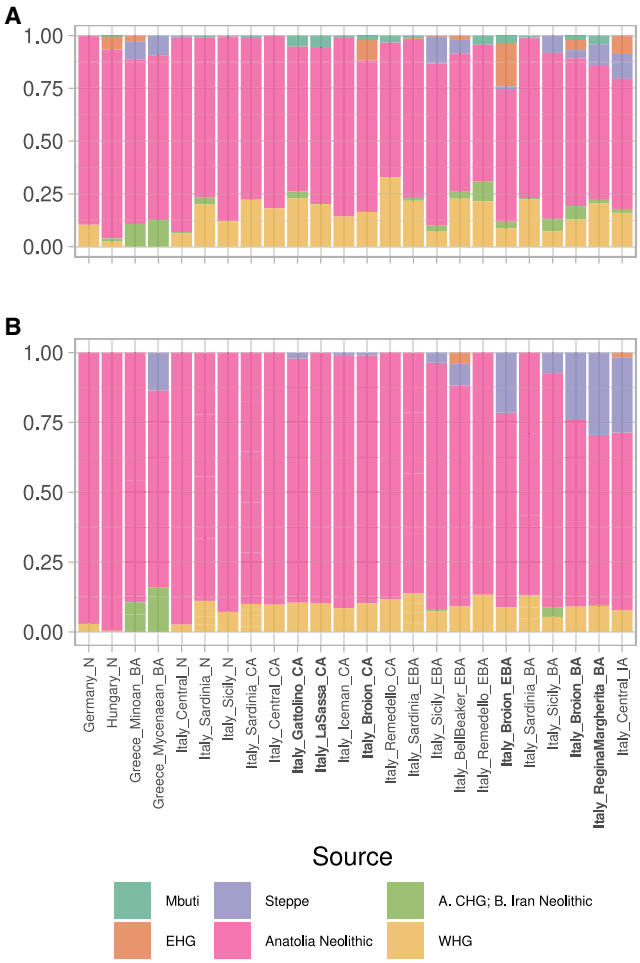

Figure 3. Ancestry composition of European and Italian ancient samples

(A) We used Chromopainter in the unlinked mode to reconstruct the genome of European (for which only a subset of relevant samples was analyzed) and Italian ancient individuals as a combination of six main putative sources. See also Figure S6.

(B) The same framework has been used on a vector composed of 4,950 different $f4$ in the form $f4$(X, Y; Target, Mbuti.DG). Mbuti.DG has not been used as a source.

See also Data S2 and S3.

also shows a high Anatolian N-like component in Sardinian and Sicilian individuals from the Chalcolithic and BA.

A separation within the EN cluster (Figure 2A) clearly differentiates Anatolian and Eastern Europe N (right) from Western Europe N, defined as samples west of Germany (left, toward western hunter-gatherer [WHG]; Data S1D). A similar separation has already been reported and interpreted as a difference in WHG proportion of these samples.[17,47–49] We note that most of our Chalcolithic individuals fall on the right side of the cluster (Anatolia and Eastern Europe).

We further explored the affinity between Italian Chalcolithic samples and WHG by computing $f4$(Mbuti.DG, Italy_Mesolithic.SG; Italy_Sardinia_N, X) (Data S2H) where X is either Italy_N, Italy_LaSassa_CA, Italy_Gattolino_CA, or Italy_Broion_CA and negative Z scores (min = −12.942; max = −3.026) indicate that Italy_Central_Mesolithic shares more with Italy_Sardinia_N than with peninsular Italian Chalcolithic. At the same time, we also tested $f4$(Mbuti.DG, Anatolia_N; Italy_Sardinia_N, X), for which only the comparison with Italy_Gattolino_CA yields significantly negative values (Z score = −3.753), suggesting that either an imbalance in WHG and Anatolia_N components between the two sides of the EN cluster or structure within the EN component[9,50] may explain our results. We note however that outgroup $f3$ statistics in the form $f3$(Mbuti.DG; Italy_CA, Y), where Italy_CA are all Chalcolithic samples from the Italian Peninsula and Y are members of the EN clusters may have no power to discriminate the observations from the PCA analysis (Data S1K). Some studies have detected an influence from groups related to hunter-gatherers from Georgia and Iran starting from the N;[13,51] however, our $f4$ of the form $f4$(Mbuti.DG, Georgia Kotias; Italy_Sardinia_N, X) is not significant for any of the pre-BA Italian groups (Data S2H).

We have evaluated the possibility of continuity at the interface between N/Chalcolithic and BA, using the qpWave/qpAdm framework (using the option "allsnps=YES"; Data S3G and S3H). When using two putative sources, all the target BA groups from North and Central Italy presented here support a scenario in which Chalcolithic-like individuals received a contribution of Steppe-related ancestry, possibly through Late N/Chalcolithic groups from the north, such as Germany Bell Beaker, France Middle N, and Italian Chalcolithic sources (Data S3G and S3H). Model-based clustering analysis (DyStruct [Figures 2B and S2] and ADMIXTURE [Figure S3])[52,53] of selected ancient and present-day individuals from Eurasia spanning from the Mesolithic to the IA points to the presence of a Steppe-related ancestry component in BA individuals from Italian Peninsula as the main difference from the Sardinian and Sicilian individuals, explaining the distribution of individuals between PN and EN in the PCA (Figure 2A).

We tested this through $f4$(Mbuti.DG, Yamnaya Kalmykia; X, Anatolia_N) (Figures 2C and S4B; Data S2B)[7,9,13,15–17,54] with X being Italian post-Mesolithic (only considering tests when at least 5,000 SNPs were available) and show that the only individuals with a significant enrichment for Steppe-related ancestry components are included within the newly generated Early BA and BA, and in published Bell Beaker (I2478 and I1979) or Italian IA individuals. Contrary to what has been previously reported for other Chalcolithic to BA transitions in Europe,[23] we also noted through outgroup $f3$ tests in form $f3$(Italian_CA/Italian_EBA_BA, ancient; Mbuti.DG) (Data S2K) that populations associated with Steppe-related ancestry did not leave a male-biased signature in Italy, which, if at all, can instead be seen through the contribution of pre-existing N groups (Figure S5).

We recapitulated the emerging picture using two orthogonal methods based on copying affinity, Chromopainter/NNLS[55] and SOURCEFIND,[56,57] and on the comparison of multiple $f4$ pairs (Figure 3). Concerning the novel samples, both approaches show an overall consistency with DyStruct (Figures 2B and S2), highlighting the post-N increase of European hunter-gatherer (HG)-related components[10,15] and the arrival of Steppe-related ancestry, with the only exception being that of Sardinia in the Early BA. Additionally, the Anatolian N and WHG proportions reported for the Italian N and Chalcolithic samples are similar

Table 2. Comparison of pairwise estimates of Chalcolithic genomes

ID1	ID2	Non-normalized P0	SE	READ relationship	*Z* upper	*Z* lower	IBD1	IBD2	Plink Fxy	Degree	Relationship
BRC013	BRC022	0.255	0.003	first degree	6.23	−13.73	0.44	0.22	0.22	first	sibling
LSC002/4	LSC011	0.266	0.002	first degree	3.37	−33.09	0.71	0.06	0.21	first	parent-offspring
LSC007	LSC002/4	0.244	0.005	first degree	4.46	−6.86					
BRC001	BRC013	0.298	0.003	second degree	2.94	−7.74	0.37	0.03	0.11	second	avuncular or grandparent-grandchild
BRC001	BRC022	0.323	0.002	unrelated	NA	−6.87	0.21	0.04	0.07	third	1st cousin

Kinship coefficient, Fxy, was estimated in PLINK 1.9.0[59] as 1/2 of the reported PIHAT value. PLINK-genome analyses used an input file of 16 imputed genomes and a total of 5,526,356 variants with MAF > 0.05 and GP > 0.99. Reported are pairs of individuals in which at least one was >0.1× coverage and who shared more than 12% of IBD. READ does not calculate third-degree relationships, rather categorizes them as "unrelated." LSC007 was too low coverage for imputation; thus, the pair with LSC002/4 was not estimated using PLINK. See also Data S4.

regardless of their position within the EN cluster identified in the PCA (Figure 2A).

We determined mitochondrial DNA (mtDNA) haplotypes for all newly generated samples (Table 1; Data S1B and S1E) and Y chromosome (Ychr) haplogroups for ten males with Ychr coverage >0.01× (Table 1; Data S1B and S1F). Consistent with the previously reported co-spread of Steppe-related ancestry and Ychr haplogroup R1,[7,10] we observed that three out of the four Italian BA males for which a Ychr haplogroup could be determined belong to haplogroup R1 and two of those were of the R1b lineage (Table 1; Data S1B and S1F). This haplogroup does not appear in the Chalcolithic samples. The two Italian R1b lineages belong to the L11 subset of R1b, which is common in modern Western Europe[58] and in ancient male Bell-Beaker burials,[9] rather than to the R1b-Z2105 varieties found in the ancient genomes from the Steppe-Belt of Russia.

Structure and mobility in the Chalcolithic and BA

The sites examined in this study include one necropolis with single burials (Gattolino, 2874–2704 BCE), and the rest are commingled cave burials (Broion, La Sassa, and Regina Margherita). Samples in this study from La Sassa are restricted to the Chalcolithic period (2850–2499 BCE) and from Regina Margherita to the BA (1609–1515 BCE). The Broion site is the only one that spans both phases: the Chalcolithic (3335–2936 BCE) and the BA (1923–1451 BCE). To better understand the site usage, whether differences are present between cave and cemetery burials and whether shifts in burial behavior occurred concurrently with shifts in genetic ancestry, we analyzed uniparental markers (informative of maternal versus paternal lineage diversity and mobility), genetic kinship (informative of mobility of family structure), and runs of homozygosity (ROHs) (which can indicate the size and homogeneity of a population).

In total, the Chalcolithic and BA sample sizes are approximately equal (n = 12 and 10, respectively), and the total number of males and females does not differ from expectations (binomial; p = 0.143); however, the ratio of males to females (7:1) within the Chalcolithic cave burials does differ from the expected value (binomial; p = 0.038), although it does not within the BA layer of Broion and Regina Margherita (5:5; binomial; p = 0.50) or in the Chalcolithic necropolis of Gattolino (2:2; binomial; p = 0.5). These results indicate a slight bias in the Chalcolithic cave burials toward males.

To identify whether first- and/or second-degree genetic kinship relationships existed among individuals within or between the four sites or between the new genomes and published ancient datasets (Data S4), we utilized two methods. First, for initial determination of kinship degrees, we utilized a pairwise mismatch estimation on the pseudo-haploid data (READ).[40] We ran the analysis on all of the newly reported ancient genomes together as one group as well as in groups by site and/or chronology (separated into N/Chalcolithic and BA) and found consistent results, regardless of grouping (Data S4A). To distinguish relationship type within degree (e.g., first degree, full siblings versus parent-offspring), we used IBD analysis as implemented in Plink-1.9[59] on imputed genotypes (STAR Methods). Genotypes were imputed using a pipeline detailed in Hui et al.[60] and STAR Methods, and in the case of close (1 to 2) degrees of relationship, both methods provided consistent results (Table 2).

We found no relationships among the seven tested BA individuals, between any of the newly presented sites, or with published data (Data S4); however, the small sample size suggests caution in inferring patterns of general validity from these individuals. For the twelve Chalcolithic individuals, close kinship relationships were detected at both cave burial sites: La Sassa and Broion and all relationships were detected between males (Tables 1 and 2). At La Sassa, the two males LSC002/004 and LSC011 have an identical Ychr haplotype (J2a-M410/J2a7-Z2397; Table 1; Data S1B and S1F), different mtDNA haplotypes (H1bv1 and J1c1; Table 1; Data S1B and S1E), a first-degree relationship, and a proportion of IBD (PI_HAT) values consistent with parent-offspring (Table 2), the summary of which indicates a father-son relationship. The nature of calibration curves for radiocarbon dating prevents the exact estimation of who is the father; however, the radiocarbon dates do not reject the relatedness inferred from aDNA (Data S1C; STAR Methods). Very low coverage sample LSC007 appears to have a first-degree relationship with LSC002/004 (Data S1B; Figure S4), and they share an identical mtDNA haplotype (H1bv1). LSC007 was too low coverage to assess the Ychr.

The chronologically contemporaneous female LSC005/013 (H1e5a) does not have any detectable close genetic kinship relationships, clusters separately from the males on the PCA, and has a strontium isotope signature that falls outside the range determined for the rest of the sampled teeth in La Sassa (n = 27; STAR Methods). To test whether LSC005/013 was genetically more similar to another population than the other La Sassa individuals, we tested $f4$(Mbuti.DG, LSC005A1_LSC013; Italy_LaSassa_CA, Other Sample/Population). There are positive non-zero Z scores for a few contemporaneous populations, however, nothing above the significance threshold (Data S2G). The summary of evidence indicates that she may not have grown up in the same local area as the other La Sassa individuals, but her genetic affinities require higher coverage and more comparative samples to be certain.

At Broion, all the individuals directly dated to the Chalcolithic (BRC001, BRC013, and BRC022) and/or that fall in the EN cluster (BRC011; Figure 2A) are males, and all of the directly dated individuals show first- and second-degree relationships (Tables 1 and 2; Data S1). These three share the Ychr G2a-P15 marker and could have the exact same haplotype (G2a3-F1193-F2291; Table 1; Data S1B and S1F); however, due to differences in coverage, the terminal branch markers are not covered in all three individuals (Data S1F). BRC013 and BRC022 share an mtDNA haplotype (H5a1; Data S1B) and have a first-degree relationship although BRC001/023 (J2a1a1) has a second-degree relationship with BRC013, but not BRC022 (Table 2). The PI_HAT values support the first-degree relationship between BRC013 and BRC022 as full siblings as well as the differing second-degree relationship between BRC013, BRC022, and BRC001/023 (Table 2). Given these values, the most parsimonious scenario is that BRC013 and BRC022 are brothers and BRC013 is the grandfather of BRC001/023; the radiocarbon dates do not reject this scenario (STAR Methods; Data S1C).

Among the 22 novel individuals, we only found two cases of matching mtDNA (Data S1B and S1E) among a variety of haplogroups associated with the N transition N1, H, J, and K,[6,10] indicating a lack of detectable structure at the mitochondrial level, which could be consistent with a larger maternal population size, exogamy, and/or with a patrilocal kinship structure across both time periods. To further explore these scenarios, we analyzed ROHs (STAR Methods) in the ancient and selected modern populations (TSI; Figures 4A–4C; Data S5C) with hapROH, which is a method to detect ROH segments in low-coverage genomes using a haplotype reference panel (STAR Methods).[61] We checked that differences in coverage did not systematically bias estimates (Figure 4D) and checked against imputation and sequencing errors (STAR Methods; Figure S7; Data S5B). We calculated segment number and length in four length categories: <1.6 centimorgan (cM); >1.6 cM; >4 cM; and >8 cM (Data S5C) and focus on the greater than 1.6 cM length category (which includes 4 and 8 cM segments), which is informative regarding recent consanguinity and is the most reliably inferred (STAR Methods; Figure S5; Data S5).

Estimates of ROH > 1.6 cM for the ancient samples after the Mesolithic[13] fall within the range of values obtained from modern Italian (TSI) individuals, suggesting similar levels of endogamy (Figures 4A and 4B; Data S5C); however, there is a significant (two-tailed t test; p = 0.0003) difference between the lengths of >1.6-cM segments in Italian N (this study and Antonio et al.[13]) and Italian BA (newly reported) and the number of >1.6-cM segments (two-tailed t test; p = 0.0001; Figure 4C; Data S5D), which is consistent with either larger effective population sizes of the BA or as the result of added diversity following an admixture event with the local Chalcolithic populations. Within the La Sassa site, individual LSC002/4 has the highest total length of >1.6-cM segments and is the only one with detected segments >8 cM (Data S5C).

Shifts in phenotypic features of ancient Italians

To determine whether the shifts in ancestry components through time corresponded to any shifts in phenotypes, we imputed genetic markers related to 115 phenotypes associated with metabolism, immunity, and pigmentation in the ancient samples presented here and in previously published studies (Data S6A–S6D; STAR Methods).[7,13,46,64,65] We analyzed a total of 332 ancient individuals (16 presented here for the first time and 316 from the literature) grouped by population: Italian Mesolithic (n = 3),[13] Italian N/Chalcolithic (n = 52; this study and Antonio et al.[13]), Italian BA (n = 60; this study, Fernandes et al.,[16] and Marcus et al.[17]), Italian IA/Modern (n = 133),[13] Near East N/Chalcolithic (n = 41),[46,64] Near East BA (n = 18),[7,46,65] and Yamnaya (n = 18; Data S6A).[4,7,64] For groups with a sample size larger than three, we calculated the frequency of the effective allele for each phenotypic variant in each population and then performed an ANOVA test to analyze shifts in the allele frequency. We compared both between Italian and non-Italian groups from different periods (Data S6B) as well as between groups within Italy, grouping the Italian individuals into 12 cohorts based both on period and geographic location (Data S6C). For both tests, we applied a Bonferroni's correction to set the significance threshold and used a Tukey test to determine the significant pairs (STAR Methods).

Eleven variants were significant when comparing the Italian groups with Near Eastern and Yamnaya populations and eight in the intra-Italy test, with four significant in both tests (Table 3; Data S6B and S6C). Although these results should be interpreted with caution due to the small sample size, some potentially interesting results emerge. For the variants that are significant in both tests (*TLR1* [rs5743618], *TNF* [rs1800629], *HLA* [rs3135388], and *SLC45A2* [rs16891982]), the signal is driven almost entirely by the post-Roman Republic Central Italy sample group (Cen_postRep), which includes Roman, Late Antiquity, and Medieval individuals. There is no detectable difference between the Italian BA samples presented here and the Italian N/Chalcolithic groups, despite the additional Steppe-related ancestry. Three out of four of the variants highlighted here are linked to protection and susceptibility to Hansen's disease (leprosy). The *HLA*-related variant (rs3135388), indicated in the susceptibility to physical manifestations of the disease in a Danish medieval population,[39] was significantly different between post-BA Italians and N/Chalcolithic Near East, BA Italians, and Yamnaya. The statistical significance of this variant in this test is probably due to the low frequency of the protective allele in central Italians from the IA onward (Data S6C). Another variant (*TNF*—rs1800629)[66] also seems to decrease in frequency of the protective allele (Table 3; Data S6C). Both results are consistent with the rise in frequency of this disease in the historical and archaeological record in Europe. The other variant, *TLR1* (rs5743618), which has been linked to both protection against leprosy[38,67] and an increased susceptibility to

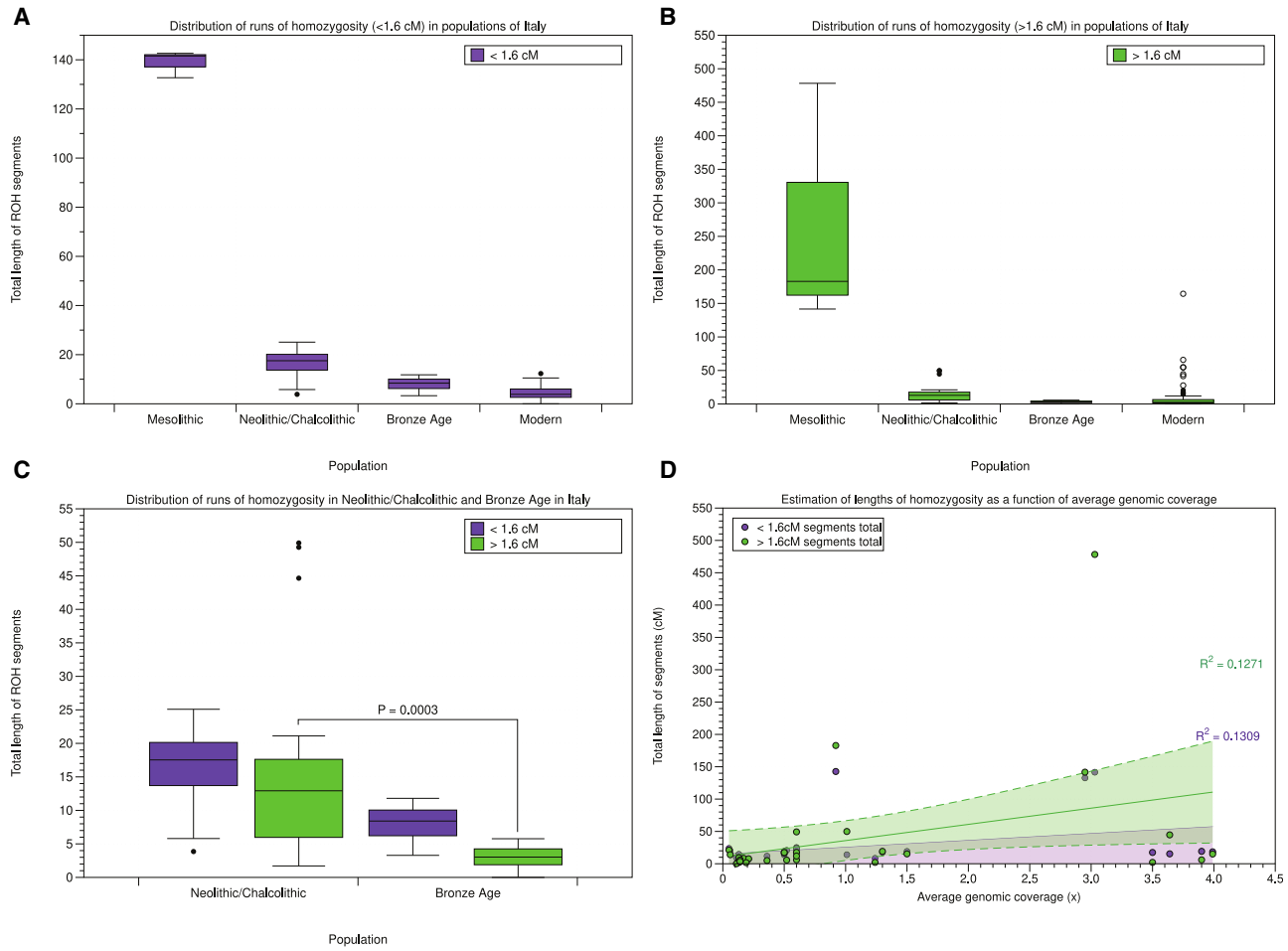

Figure 4. Runs of homozygosity in ancient and modern populations of the Italian Peninsula

(A) Distribution of total length of segments <1.6 centimorgan (cM) in Mesolithic,[13] Neolithic/Chalcolithic (Antonio et al.[13] and this study), Bronze Age (this study), and Modern Italians (TSI).[62]

(B) Distribution of total length of segments >1.6 cM in Mesolithic,[13] Neolithic/Chalcolithic (Antonio et al.[13] and this study), Bronze Age (this study), and Modern Italians (TSI).[62]

(C) Distribution of the total length of segments <1.6 cM (purple) and >1.6 cM (green) in Neolithic/Chalcolithic (Antonio et al.[13] and this study) and Bronze Age (this study).

(D) Total lengths of segments <1.6 cM (purple) and >1.6 cM (green) in all ancient samples (Antonio et al.[13] and this study) plotted against the average genomic coverage. Linear regression fitted by Datagraph (http://visualdatatools.com),[63] solid line is the fitted line, and shaded area represents 95% confidence interval. R^2 values are color coded to match the legend and reported in the lower right-hand corner.

See also Data S5.

tuberculosis in Asian populations,[68] shows a significant result in the other direction, driven by higher frequency only in the post-Roman Republic Central Italy group (Table 3; Data S6C).

The fourth variant significant in both tests (rs16891982 in *SLC45A2* gene) is implicated in hair and eye pigmentation. In terms of physical appearance, both the Chalcolithic and BA Italy groups have imputed phenotypes more similar to IA and Later Romans than to earlier populations in Italy and the Near East. The three previously published Mesolithic individuals from Italy[13,27,29] are predicted to have dark skin, dark hair, and blue eyes (Data S6D), although most of the other samples have predicted intermediate skin pigmentation, brown hair, and brown eyes; however, individuals with blue eyes paired with either dark or blond hair are also predicted in all time periods except in the N individuals from Central Italy (Data S6D).[13] The variant rs16891982, linked to darker eyes and hair, shows a significant difference between post-BA Italy group and previous groups from Italy, with the frequency decreasing in Central Italy starting in the newly reported Chalcolithic individuals and with the lowest values observed for the newly reported BA individuals and the post-Roman Republic Central Italy group. This difference is particularly notable compared to N Central Italy and Sardinian groups prior to the BA (Data S6C).

DISCUSSION

The newly generated genomes provide a more detailed description of demographic dynamics of later Italian prehistory in a

Table 3. List of significant phenotypic variants

SNP	Gene	Phenotype	Comparison between Italy, Near East, and Yamnaya significance	Significant pairs of groups	Intra-Italy comparison significance	Significant pairs of groups
rs2167079	*NR1H3, ACP2*	HDL +	y	Yam[a] versus all except NE_BA		
rs174546	*FADS1/ FADS2*	LDL +	y	Ita_postBA versus NE_NeoCA and Yam[a]		
rs174570	*FADS1*vs.3	LDL +;HDL +;TG −	y	Yam versus NE_BA and Ita_postBA[a]; Ita_NeoCA versus Ita_postBA		
rs5743618	*TLR1*	protective factor for leprosy	y	Ita_postBA[a] versus Ita_NeoCA, NE_NeoCA, Ita_BA	y	Cen_postRep[a] versus Cen_NeoCA, Sic_Neo, Sar_CA, Sic_BA, Sar_BANur, Sar_IAPun, Cen_IARep
rs1800629	*TNF*	protective factor for leprosy	y	Ita_postBA versus Ita_NeoCA and NE_NeoCA[a]	y	Cen_postRep versus CA[a], Sar_BANur
rs3135388	*HLA*	protective factor for leprosy	y	Ita_postBA versus NE_NeoCA[a], Ita_BA, Yam	y	Sar_BANur[a] versus Cen_IARep, Cen_postRep; Sar_CA versus Cen_IARep
rs4251545	*IRAK4*	risk factor for Gram-positive infection			y	not significant pairs
rs13119723	intronic	protective factor for celiac disease	y	Yam[a] versus all Ita		
rs2187668	*HLA-DQA1*	risk factor for celiac disease and gluten intolerance	y	NE_NeoCA and Yam[a] versus all Ita		
rs7775228	*HLA-DRA*	risk factor for celiac disease and gluten intolerance			y	BA[a] versus Sar_Neo and all Cen
rs4713586	*HLA-DRA*	risk factor for celiac disease and gluten intolerance			y	BA versus all except CA[b]
rs1050152	*SLC22A4*	risk factor for Crohn's disease	y	NE_NeoCA versus Ita_BA[a] and Ita_postBA		
rs16891982	*SLC45A2*	eye color: brown; hair color: black versus nonvs.black	y	Ita_postBA versus NE_NeoCA, Ita_NeoCA[a], Ita_BA	y	Cen_postRep versus Cen_NeoCA[a], Sar_CA, Sar_BANur
rs28777	*SLC45A2*	hair color: AAvs.black/CCvs.red; skin color: dark	y	Ita_postBA versus Ita_NeoCA[a], Ita_BA		
rs1426654	*SLC24A5*	skin color: intermediate			y	Cen_NeoCA[a] versus all

See also Data S6. BA, Bronze Age; CA, Chalcolithic; Cen, Central Italians; IA, Iron Age; Ita, Italy; NE, Near East; Neo, Neolithic; Nur, Nuragic; Pun, Punic; Rep, Republic; Sar, Sardinia; Sic, Sicily; SNP, variantID; Yam, Yamnaya.

[a]The groups with the highest frequency of the effective allele in the significant pairs

[b]Frequency approaching 1 in most groups, except BA and CA

European context.[7,9,11,13] The split among European Early N individuals into two groups observed in the PCA and already reported in Marcus et al.[17] separates Sardinia N from mainland Italy, coupled with the higher affinity of the Sardinia N to both Anatolia_N and WHG, raise the possibility of population structure within the EN component, although deeper analysis, including high-coverage ancient genomes, is needed to dissect subtle differences in ancestry.

Our analyses show the expected signature of peri- and post-BA movements from Steppe-related populations across Italy: absent in Italian individuals from the N and Chalcolithic, emerging in the Early BA (Italian Bell Beaker [I2478: 2195–1940 calBCE],[9] Italian Remedello [RISE486: 2134–1773 calBCE],[7,13] and Broion [BRC010: 1952–1752 calBCE (95.4%)]) and increasing through time in the individuals from Broion and Regina Margherita (GCP003: 1626–1497 calBCE [95.4%]). These samples confirm the date of arrival in Northern Italy to at least ~2000 BCE and its presence in Central Italy by 4 centuries later, although denser sampling strategies are needed to assess the dynamics of this spread. Our qpAdm results suggest that the Steppe-related ancestry component could have arrived through Late N/Bell Beaker groups from Central Europe, though what remains unknown due to small sample size and limited geographical and chronological distribution is whether there were multiple Steppe population sources and the exact timing and diffusion of this ancestry component through the Italian Peninsula. The R1b subtype found in BA Broion is a lineage found in both ancient Sicilian samples and Italian Bell Beakers. Together with the autosomal affinity of North and Central Italian BA groups with Late N Germany, the Ychr data point to a possibly Northern-, transalpine-, and potentially Bell-Beaker-associated source of the Italian Steppe-related ancestry.

The importance of male kinship structures in the interface between the Chalcolithic and BA has also been explored using our autosomal data. It has long been assumed that the commingled cave burials of the Chalcolithic included some form of kinship structure; however, it was not possible to directly reveal it before the advent of aDNA. Here, we see the pattern that, in the Chalcolithic period, these locations were preferentially used to bury closely related male individuals, though the social significance of this fact is not clear. Although the Chalcolithic populations of Italy utilized natural burial chamber spaces, rock-cut tombs, and trench graves more than building megalithic monuments of the kind seen along the Atlantic Façade in an earlier time period, it appears that the importance of burying related males together is a shared feature. The genetic evidence shown here is consistent with an emphasis on patrilineal descendancy and patrilocality for these burial rites to the populations at both La Sassa and Broion, an emphasis that disappears in the BA but is also not present at the single-burial style Chalcolithic cemetery of Gattolino (possibly due to small sample size). It is important to note that these sites do not represent a random and unbiased sampling of the local populations, rather a snapshot of one particular ritual aspect of these societies; thus, it cannot be inferred whether patrilocality and patrilineality were generally practiced or whether these patterns changed over time. More sampling for genetics and isotopes is needed to reconstruct the general population structure and inter-community relationships.

The arrival of the Steppe-related ancestry does not seem to have affected the frequency patterns of any of the phenotypes assessed in this work. Rather, the biggest changes seem to have occurred with or after the Roman Imperial period. The decrease in alleles associated with a protection against leprosy after the IA is potentially interesting, given the increase in manifestations of the disease in the European bioarchaeological and historical record from the 3rd to 4th millennium BCE[69] until its decline around the 1st millennium CE.[70] It is still not clear exactly how these variants interact with the disease and other pathogenic mycobacterial infections; thus, more work is needed on the clinical side before the full evolutionary history can be determined. It is also important to note that, as we did not test all possible phenotypes but only a small subset, our results are likely to be not the only phenotypic differences and more work must be done to fully understand the complex relationships between evolutionary mechanisms and human genes. Fortunately, whole ancient genomes like those generated in this study provide an invaluable resource that can be revisited in light of advancements in all areas of biology and genetics.

STAR★METHODS

Detailed methods are provided in the online version of this paper and include the following:

- KEY RESOURCES TABLE
- RESOURCE AVAILABILITY
  - Lead contact
  - Materials availability
  - Data and code availability
- EXPERIMENTAL MODEL AND SUBJECT DETAILS
  - Grottina dei Covoloni del Broion
  - Grotta La Sassa
  - Necropoli di Gattolino di Cesena
  - Radiocarbon method and date of Gattolino
  - Grotta Regina Margherita
  - Sample B297 comes from Sounding D, Context 32
  - Samples B152 and B154 come from Sounding E, Context 60
- METHOD DETAILS
  - DNA extraction
  - Library preparation
  - DNA sequencing
- QUANTIFICATION AND STATISTICAL ANALYSIS
  - Mapping
  - aDNA authentication
  - Calculating genetic sex estimation
  - Determining mtDNA haplogroups
  - Y chromosome variant calling and haplotyping
  - Kinship analysis and identical samples
  - Identifying kinship in new samples
  - Preparing the datasets for autosomal analysis
  - Principal component analysis
  - DyStruct
  - $f4$ statistics
  - Outgroup f3 statistics
  - Admixture analysis
  - Chromopainter/NNLS and SourceFind

- f4 NNLS analysis
- qpAdm
- Genome imputation
- Runs of Homozygosity
- Predicting imputation errors
- Introducing imputation errors into modern genomes
- Detecting ROH segments in ancient genomes
- Phenotype prediction

SUPPLEMENTAL INFORMATION

Supplemental information can be found online at https://doi.org/10.1016/j.cub.2021.04.022.

ACKNOWLEDGMENTS

This work is supported by European Union through the European Regional Development Fund (project no. 2014–2020.4.01.16–0030; C.L.S., T.S., F.M., and M.M.) and the Estonian Research Council personal research grant (PRG243; C.L.S. and M.M.). This research was additionally supported by the European Union through the European Regional Development Fund (Project No. 2014-2020.4.01.15-0012; M.M.) and European Union through Horizon 2020 grant no. 810645 (M.M.). C.C. was supported for this project by St. Hugh's College via a Jackie Lambert Research Grant. E.D. was supported by Sapienza University of Rome fellowship "borsa di studio per attività di perfezionamento all'estero 2017." L.P. was supported by UniPd PRID 2019 and by European Regional Development Fund project no. 2014-2020.4.01.16-0024, MOBTT53. R.H. was supported by the Wellcome Trust (award no. 2000368/Z/15/Z). T.K. is supported by KU Leuven startup grant STG/18/021. S.T. is funded by the European Research Council under the European Union's Horizon 2020 Research and Innovation Programme (grant agreement no. 803147-951 RESOLUTION; https://site.unibo.it/resolution-erc/en). S.B. is supported by ERC no. 724046 – SUCCESS; http://www.erc-success.eu/. R.S. is funded by the British Academy (SG140575). L.A. was supported by the Netherlands Organisation for Scientific Research (NWO) Free Competition grant 360-61-060. A.D. contributed sequencing funds via the Faculty Research Fund of the Faculty of Humanities and Social Sciences, Newcastle University. We thank the other members of the Estonian Biocentre and aDNA group, including Lehti Saag, for their expertise and Paula Reimer and the 14Chrono Centre at Queen's University Belfast for assistance with the radiocarbon dates.

AUTHOR CONTRIBUTIONS

Conceptualization, C.L.S., L.P., C.C., T.S., and F.M.; investigation, T.S., G.L., and O.L. (aDNA); I.A. (isotopes); and S.T. (radiocarbon); resources, N.C., C.S., L.P., C.C., S.B., M.F.R., F.D.A., L.S., L.A., and R.S.; formal analysis, T.S., F.M., C.L.S., T.K., E.D., R.H., and L.P.; writing – original draft, T.S., F.M., L.P., and C.L.S.; writing – review & editing, all authors; funding acquisition, A.D., L.P., and M.M.; supervision, C.L.S., L.P., and F.M.

DECLARATION OF INTERESTS

The authors declare no competing interests.

Received: April 10, 2020
Revised: November 28, 2020
Accepted: April 9, 2021
Published: May 10, 2021

REFERENCES

1. Pearce, M. (2019). The "copper age"—a history of the concept. J. World Prehist. *32*, 229–250.
2. Dolfini, A. (2020). From the Neolithic to the Bronze Age in Central Italy: settlement, burial, and social change at the dawn of metal production. J. Archaeol. Res. *28*, 503–556.
3. Skoglund, P., Malmström, H., Raghavan, M., Storå, J., Hall, P., Willerslev, E., Gilbert, M.T.P., Götherström, A., and Jakobsson, M. (2012). Origins and genetic legacy of Neolithic farmers and hunter-gatherers in Europe. Science *336*, 466–469.
4. Mathieson, I., Alpaslan-Roodenberg, S., Posth, C., Szécsényi-Nagy, A., Rohland, N., Mallick, S., Olalde, I., Broomandkhoshbacht, N., Candilio, F., Cheronet, O., et al. (2018). The genomic history of southeastern Europe. Nature *555*, 197–203.
5. Hofmanová, Z., Kreutzer, S., Hellenthal, G., Sell, C., Diekmann, Y., Díez-Del-Molino, D., van Dorp, L., López, S., Kousathanas, A., Link, V., et al. (2016). Early farmers from across Europe directly descended from Neolithic Aegeans. Proc. Natl. Acad. Sci. USA *113*, 6886–6891.
6. Lazaridis, I., Patterson, N., Mittnik, A., Renaud, G., Mallick, S., Kirsanow, K., Sudmant, P.H., Schraiber, J.G., Castellano, S., Lipson, M., et al. (2014). Ancient human genomes suggest three ancestral populations for present-day Europeans. Nature *513*, 409–413.
7. Allentoft, M.E., Sikora, M., Sjögren, K.-G., Rasmussen, S., Rasmussen, M., Stenderup, J., Damgaard, P.B., Schroeder, H., Ahlström, T., Vinner, L., et al. (2015). Population genomics of Bronze Age Eurasia. Nature *522*, 167–172.
8. Olalde, I., Mallick, S., Patterson, N., Rohland, N., Villalba-Mouco, V., Silva, M., Dulias, K., Edwards, C.J., Gandini, F., Pala, M., et al. (2019). The genomic history of the Iberian Peninsula over the past 8000 years. Science *363*, 1230–1234.
9. Olalde, I., Brace, S., Allentoft, M.E., Armit, I., Kristiansen, K., Booth, T., Rohland, N., Mallick, S., Szécsényi-Nagy, A., Mittnik, A., et al. (2018). The Beaker phenomenon and the genomic transformation of northwest Europe. Nature *555*, 190–196.
10. Haak, W., Lazaridis, I., Patterson, N., Rohland, N., Mallick, S., Llamas, B., Brandt, G., Nordenfelt, S., Harney, E., Stewardson, K., et al. (2015). Massive migration from the steppe was a source for Indo-European languages in Europe. Nature *522*, 207–211.
11. Raveane, A., Aneli, S., Montinaro, F., Athanasiadis, G., Barlera, S., Birolo, G., Boncoraglio, G., Di Blasio, A.M., Di Gaetano, C., Pagani, L., et al. (2019). Population structure of modern-day Italians reveals patterns of ancient and archaic ancestries in Southern Europe. Sci. Adv. *5*, eaaw3492.
12. Lazaridis, I., Mittnik, A., Patterson, N., Mallick, S., Rohland, N., Pfrengle, S., Furtwängler, A., Peltzer, A., Posth, C., Vasilakis, A., et al. (2017). Genetic origins of the Minoans and Mycenaeans. Nature *548*, 214–218.
13. Antonio, M.L., Gao, Z., Moots, H.M., Lucci, M., Candilio, F., Sawyer, S., Oberreiter, V., Calderon, D., Devitofranceschi, K., Aikens, R.C., et al. (2019). Ancient Rome: a genetic crossroads of Europe and the Mediterranean. Science *366*, 708–714.
14. Keller, A., Graefen, A., Ball, M., Matzas, M., Boisguerin, V., Maixner, F., Leidinger, P., Backes, C., Khairat, R., Forster, M., et al. (2012). New insights into the Tyrolean Iceman's origin and phenotype as inferred by whole-genome sequencing. Nat. Commun. *3*, 698.
15. Fu, Q., Posth, C., Hajdinjak, M., Petr, M., Mallick, S., Fernandes, D., Furtwängler, A., Haak, W., Meyer, M., Mittnik, A., et al. (2016). The genetic history of Ice Age Europe. Nature *534*, 200–205.
16. Fernandes, D.M., Mittnik, A., Olalde, I., Lazaridis, I., Cheronet, O., Rohland, N., Mallick, S., Bernardos, R., Broomandkhoshbacht, N., Carlsson, J., et al. (2020). The spread of steppe and Iranian-related ancestry in the islands of the western Mediterranean. Nat. Ecol. Evol. *4*, 334–345.
17. Marcus, J.H., Posth, C., Ringbauer, H., Lai, L., Skeates, R., Sidore, C., Beckett, J., Furtwängler, A., Olivieri, A., Chiang, C.W.K., et al. (2020). Genetic history from the Middle Neolithic to present on the Mediterranean island of Sardinia. Nat. Commun. *11*, 939.
18. Mittnik, A., Massy, K., Knipper, C., Wittenborn, F., Friedrich, R., Pfrengle, S., Burri, M., Carlichi-Witjes, N., Deeg, H., Furtwängler, A., et al. (2019). Kinship-based social inequality in Bronze Age Europe. Science *366*, 731–734.

19. Schroeder, H., Margaryan, A., Szmyt, M., Theulot, B., Włodarczak, P., Rasmussen, S., Gopalakrishnan, S., Szczepanek, A., Konopka, T., Jensen, T.Z.T., et al. (2019). Unraveling ancestry, kinship, and violence in a Late Neolithic mass grave. Proc. Natl. Acad. Sci. USA *116*, 10705–10710.

20. Racimo, F., Sikora, M., Vander Linden, M., Schroeder, H., and Lalueza-Fox, C. (2020). Beyond broad strokes: sociocultural insights from the study of ancient genomes. Nat. Rev. Genet. *21*, 355–366.

21. Sánchez-Quinto, F., Malmström, H., Fraser, M., Girdland-Flink, L., Svensson, E.M., Simões, L.G., George, R., Hollfelder, N., Burenhult, G., Noble, G., et al. (2019). Megalithic tombs in western and northern Neolithic Europe were linked to a kindred society. Proc. Natl. Acad. Sci. USA *116*, 9469–9474.

22. Scheib, C.L., Hui, R., D'Atanasio, E., Wohns, A.W., Inskip, S.A., Rose, A., Cessford, C., O'Connell, T.C., Robb, J.E., Evans, C., et al. (2019). East Anglian early Neolithic monument burial linked to contemporary Megaliths. Ann. Hum. Biol. *46*, 145–149.

23. Saag, L., Varul, L., Scheib, C.L., Stenderup, J., Allentoft, M.E., Saag, L., Pagani, L., Reidla, M., Tambets, K., Metspalu, E., et al. (2017). Extensive farming in Estonia started through a sex-biased migration from the Steppe. Curr. Biol. *27*, 2185–2193.e6.

24. Martiniano, R., Cassidy, L.M., Ó'Maoldúin, R., McLaughlin, R., Silva, N.M., Manco, L., Fidalgo, D., Pereira, T., Coelho, M.J., Serra, M., et al. (2017). The population genomics of archaeological transition in west Iberia: Investigation of ancient substructure using imputation and haplotype-based methods. PLoS Genet. *13*, e1006852.

25. Knipper, C., Mittnik, A., Massy, K., Kociumaka, C., Kucukkalipci, I., Maus, M., Wittenborn, F., Metz, S.E., Staskiewicz, A., Krause, J., and Stockhammer, P.W. (2017). Female exogamy and gene pool diversification at the transition from the Final Neolithic to the Early Bronze Age in central Europe. Proc. Natl. Acad. Sci. USA *114*, 10083–10088.

26. Furholt, M. (2019). Re-integrating archaeology: a contribution to aDNA studies and the migration discourse on the 3rd millennium BC in Europe. Proc. Prehist. Soc. *85*, 115–129.

27. Olalde, I., Allentoft, M.E., Sánchez-Quinto, F., Santpere, G., Chiang, C.W.K., DeGiorgio, M., Prado-Martinez, J., Rodríguez, J.A., Rasmussen, S., Quilez, J., et al. (2014). Derived immune and ancestral pigmentation alleles in a 7,000-year-old Mesolithic European. Nature *507*, 225–228.

28. Brace, S., Diekmann, Y., Booth, T.J., van Dorp, L., Faltyskova, Z., Rohland, N., Mallick, S., Olalde, I., Ferry, M., Michel, M., et al. (2019). Ancient genomes indicate population replacement in Early Neolithic Britain. Nat. Ecol. Evol. *3*, 765–771.

29. Saag, L., Laneman, M., Varul, L., Malve, M., Valk, H., Razzak, M.A., Shirobokov, I.G., Khartanovich, V.I., Mikhaylova, E.R., Kushniarevich, A., et al. (2019). The arrival of Siberian ancestry connecting the Eastern Baltic to Uralic speakers further East. Curr. Biol. *29*, 1701–1711.e16.

30. Wilde, S., Timpson, A., Kirsanow, K., Kaiser, E., Kayser, M., Unterländer, M., Hollfelder, N., Potekhina, I.D., Schier, W., Thomas, M.G., and Burger, J. (2014). Direct evidence for positive selection of skin, hair, and eye pigmentation in Europeans during the last 5,000 y. Proc. Natl. Acad. Sci. USA *111*, 4832–4837.

31. Mathieson, S., and Mathieson, I. (2018). FADS1 and the timing of human adaptation to agriculture. Mol. Biol. Evol. *35*, 2957–2970.

32. Roberts, C.A., Lewis, M.E., and Manchester, K. (2002). The past and present of leprosy: archaeological, historical, palaeopathological and clinical approaches. In Proceedings of the 3rd International Congress on the Evolution and Palaeoepidemiology of the Infectious Diseases, ICEPID, 26-31 July 1999, University of Bradford, C.A. Roberts, et al., eds. (Archaeopress).

33. Mariotti, V., Dutour, O., Belcastro, M.G., Facchini, F., and Brasili, P. (2005). Probable early presence of leprosy in Europe in a Celtic skeleton of the 4th-3rd century BC (Casalecchio di Reno, Bologna, Italy). Int. J. Osteoarchaeol. *15*, 311–325.

34. Kalisch, P.A. (1975). An overview of research on the history of leprosy. Part 1. From Celsus to Simpson, Circa. 1 AD Part 2. From Virchow to Møller-Christense, 1845-1973. Int. J. Lepr. Other Mycobact. Dis. *43*, 129–144.

35. Schuring, R.P., Hamann, L., Faber, W.R., Pahan, D., Richardus, J.H., Schumann, R.R., and Oskam, L. (2009). Polymorphism N248S in the human Toll-like receptor 1 gene is related to leprosy and leprosy reactions. J. Infect. Dis. *199*, 1816–1819.

36. Wong, S.H., Gochhait, S., Malhotra, D., Pettersson, F.H., Teo, Y.Y., Khor, C.C., Rautanen, A., Chapman, S.J., Mills, T.C., Srivastava, A., et al. (2010). Leprosy and the adaptation of human toll-like receptor 1. PLoS Pathog. *6*, e1000979.

37. Sapkota, B.R., Macdonald, M., Berrington, W.R., Misch, E.A., Ranjit, C., Siddiqui, M.R., Kaplan, G., and Hawn, T.R. (2010). Association of TNF, MBL, and VDR polymorphisms with leprosy phenotypes. Hum. Immunol. *71*, 992–998.

38. Misch, E.A., Macdonald, M., Ranjit, C., Sapkota, B.R., Wells, R.D., Siddiqui, M.R., Kaplan, G., and Hawn, T.R. (2008). Human TLR1 deficiency is associated with impaired mycobacterial signaling and protection from leprosy reversal reaction. PLoS Negl. Trop. Dis. *2*, e231.

39. Krause-Kyora, B., Nutsua, M., Boehme, L., Pierini, F., Pedersen, D.D., Kornell, S.-C., Drichel, D., Bonazzi, M., Möbus, L., Tarp, P., et al. (2018). Ancient DNA study reveals HLA susceptibility locus for leprosy in medieval Europeans. Nat. Commun. *9*, 1569.

40. Monroy Kuhn, J.M., Jakobsson, M., and Günther, T. (2018). Estimating genetic kin relationships in prehistoric populations. PLoS ONE *13*, e0195491.

41. Reimer, P.J., Austin, W.E.N., Bard, E., Bayliss, A., Blackwell, P.G., Ramsey, C.B., Butzin, M., Cheng, H., Lawrence Edwards, R., Friedrich, M., et al. (2020). The IntCal20 Northern Hemisphere Radiocarbon Age Calibration Curve (0–55 cal kBP). Radiocarbon *62*, 725–757.

42. Stuiver, M., Reimer, P.J., and Reimer, R.W. (2021). CABLIB 8.2. http://calib.org/calib/.

43. Ramsey, C.B. (2009). Bayesian analysis of radiocarbon dates. Radiocarbon *51*, 337–360.

44. Patterson, N., Price, A.L., and Reich, D. (2006). Population structure and eigenanalysis. PLoS Genet. *2*, e190.

45. Price, A.L., Patterson, N.J., Plenge, R.M., Weinblatt, M.E., Shadick, N.A., and Reich, D. (2006). Principal components analysis corrects for stratification in genome-wide association studies. Nat. Genet. *38*, 904–909.

46. Lazaridis, I., Nadel, D., Rollefson, G., Merrett, D.C., Rohland, N., Mallick, S., Fernandes, D., Novak, M., Gamarra, B., Sirak, K., et al. (2016). Genomic insights into the origin of farming in the ancient Near East. Nature *536*, 419–424.

47. Lipson, M., Szécsényi-Nagy, A., Mallick, S., Pósa, A., Stégmár, B., Keerl, V., Rohland, N., Stewardson, K., Ferry, M., Michel, M., et al. (2017). Parallel palaeogenomic transects reveal complex genetic history of early European farmers. Nature *551*, 368–372.

48. Brunel, S., Bennett, E.A., Cardin, L., Garraud, D., Barrand Emam, H., Beylier, A., Boulestin, B., Chenal, F., Ciesielski, E., Convertini, F., et al. (2020). Ancient genomes from present-day France unveil 7,000 years of its demographic history. Proc. Natl. Acad. Sci. USA *117*, 12791–12798.

49. Rivollat, M., Jeong, C., Schiffels, S., Küçükkalıpçı, İ., Pemonge, M.-H., Rohrlach, A.B., Alt, K.W., Binder, D., Friederich, S., Ghesquière, E., et al. (2020). Ancient genome-wide DNA from France highlights the complexity of interactions between Mesolithic hunter-gatherers and Neolithic farmers. Sci. Adv. *6*, eaaz5344.

50. Shennan, S. (2018). The First Farmers of Europe: An Evolutionary Perspective (Cambridge University Press).

51. Sarno, S., Boattini, A., Pagani, L., Sazzini, M., De Fanti, S., Quagliariello, A., Gnecchi Ruscone, G.A., Guichard, E., Ciani, G., Bortolini, E., et al. (2017). Ancient and recent admixture layers in Sicily and Southern Italy

trace multiple migration routes along the Mediterranean. Sci. Rep. *7*, 1984.

52. Joseph, T.A., and Pe'er, I. (2019). Inference of population structure from time-series genotype data. Am. J. Hum. Genet. *105*, 317–333.
53. Alexander, D.H., Novembre, J., and Lange, K. (2009). Fast model-based estimation of ancestry in unrelated individuals. Genome Res. *19*, 1655–1664.
54. Sikora, M., Carpenter, M.L., Moreno-Estrada, A., Henn, B.M., Underhill, P.A., Sánchez-Quinto, F., Zara, I., Pitzalis, M., Sidore, C., Busonero, F., et al. (2014). Population genomic analysis of ancient and modern genomes yields new insights into the genetic ancestry of the Tyrolean Iceman and the genetic structure of Europe. PLoS Genet. *10*, e1004353.
55. Lawson, D.J., Hellenthal, G., Myers, S., and Falush, D. (2012). Inference of population structure using dense haplotype data. PLoS Genet. *8*, e1002453.
56. Chacón-Duque, J.-C., Adhikari, K., Fuentes-Guajardo, M., Mendoza-Revilla, J., Acuña-Alonzo, V., Barquera, R., Quinto-Sánchez, M., Gómez-Valdés, J., Everardo Martínez, P., Villamil-Ramírez, H., et al. (2018). Latin Americans show wide-spread Converso ancestry and imprint of local Native ancestry on physical appearance. Nat. Commun. *9*, 5388.
57. Ongaro, L., Scliar, M.O., Flores, R., Raveane, A., Marnetto, D., Sarno, S., Gnecchi-Ruscone, G.A., Alarcón-Riquelme, M.E., Patin, E., Wangkumhang, P., et al. (2019). The genomic impact of European colonization of the Americas. Curr. Biol. *29*, 3974–3986.e4.
58. Kivisild, T. (2017). The study of human Y chromosome variation through ancient DNA. Hum. Genet. *136*, 529–546.
59. Chang, C.C., Chow, C.C., Tellier, L.C., Vattikuti, S., Purcell, S.M., and Lee, J.J. (2015). Second-generation PLINK: rising to the challenge of larger and richer datasets. Gigascience *4*, 7.
60. Hui, R., D'Atanasio, E., Cassidy, L.M., Scheib, C.L., and Kivisild, T. (2020). Evaluating genotype imputation pipeline for ultra-low coverage ancient genomes. Sci. Rep. *10*, 18542.
61. Ringbauer, H., Novembre, J., and Steinrücken, M. (2020). Human parental relatedness through time - detecting runs of homozygosity in ancient DNA. bioRxiv. https://doi.org/10.1101/2020.05.31.126912.
62. The 1000 Genomes Project Consortium (2015). A global reference for human genetic variation. Nature *526*, 68–74.
63. MacAskill, M.R. (2012). DataGraph 3.0. J. Statist. Softw. Softw. Rev. *47*, 1–9.
64. Mathieson, I., Lazaridis, I., Rohland, N., Mallick, S., Patterson, N., Roodenberg, S.A., Harney, E., Stewardson, K., Fernandes, D., Novak, M., et al. (2015). Genome-wide patterns of selection in 230 ancient Eurasians. Nature *528*, 499–503.
65. Damgaard, P.B., Marchi, N., Rasmussen, S., Peyrot, M., Renaud, G., Korneliussen, T., Moreno-Mayar, J.V., Pedersen, M.W., Goldberg, A., Usmanova, E., et al. (2018). 137 ancient human genomes from across the Eurasian steppes. Nature *557*, 369–374.
66. Zhang, F.-R., Huang, W., Chen, S.-M., Sun, L.-D., Liu, H., Li, Y., Cui, Y., Yan, X.-X., Yang, H.-T., Yang, R.-D., et al. (2009). Genomewide association study of leprosy. N. Engl. J. Med. *361*, 2609–2618.
67. Johnson, C.M., Lyle, E.A., Omueti, K.O., Stepensky, V.A., Yegin, O., Alpsoy, E., Hamann, L., Schumann, R.R., and Tapping, R.I. (2007). Cutting edge: a common polymorphism impairs cell surface trafficking and functional responses of TLR1 but protects against leprosy. J. Immunol. *178*, 7520–7524.
68. Qi, H., Sun, L., Wu, X., Jin, Y., Xiao, J., Wang, S., Shen, C., Chu, P., Qi, Z., Xu, F., et al. (2015). Toll-like receptor 1(TLR1) gene SNP rs5743618 is associated with increased risk for tuberculosis in Han Chinese children. Tuberculosis (Edinb.) *95*, 197–203.
69. Köhler, K., Marcsik, A., Zádori, P., Biro, G., Szeniczey, T., Fábián, S., Serlegi, G., Marton, T., Donoghue, H.D., and Hajdu, T. (2017). Possible cases of leprosy from the Late Copper Age (3780-3650 cal BC) in Hungary. PLoS ONE *12*, e0185966.
70. Donoghue, H.D., Marcsik, A., Matheson, C., Vernon, K., Nuorala, E., Molto, J.E., Greenblatt, C.L., and Spigelman, M. (2005). Co-infection of Mycobacterium tuberculosis and Mycobacterium leprae in human archaeological samples: a possible explanation for the historical decline of leprosy. Proc. Biol. Sci. *272*, 389–394.
71. Behar, D.M., van Oven, M., Rosset, S., Metspalu, M., Loogväli, E.-L., Silva, N.M., Kivisild, T., Torroni, A., and Villems, R. (2012). A "Copernican" reassessment of the human mitochondrial DNA tree from its root. Am. J. Hum. Genet. *90*, 675–684.
72. McCarthy, S., Das, S., Kretzschmar, W., Delaneau, O., Wood, A.R., Teumer, A., Kang, H.M., Fuchsberger, C., Danecek, P., Sharp, K., et al.; Haplotype Reference Consortium (2016). A reference panel of 64,976 haplotypes for genotype imputation. Nat. Genet. *48*, 1279–1283.
73. Meyer, M., and Kircher, M. (2010). Illumina sequencing library preparation for highly multiplexed target capture and sequencing. Cold Spring Harb. Protoc. *2010*, pdb.prot5448.
74. Martin, M. (2011). Cutadapt removes adapter sequences from high-throughput sequencing reads. EMBnet. J. *17*, 10–12.
75. Li, H., and Durbin, R. (2009). Fast and accurate short read alignment with Burrows-Wheeler transform. Bioinformatics *25*, 1754–1760.
76. Li, H., Handsaker, B., Wysoker, A., Fennell, T., Ruan, J., Homer, N., Marth, G., Abecasis, G., and Durbin, R.; 1000 Genome Project Data Processing Subgroup (2009). The Sequence Alignment/Map format and SAMtools. Bioinformatics *25*, 2078–2079.
77. DePristo, M.A., Banks, E., Poplin, R., Garimella, K.V., Maguire, J.R., Hartl, C., Philippakis, A.A., del Angel, G., Rivas, M.A., Hanna, M., et al. (2011). A framework for variation discovery and genotyping using next-generation DNA sequencing data. Nat. Genet. *43*, 491–498.
78. Jónsson, H., Ginolhac, A., Schubert, M., Johnson, P.L.F., and Orlando, L. (2013). mapDamage2.0: fast approximate Bayesian estimates of ancient DNA damage parameters. Bioinformatics *29*, 1682–1684.
79. Jones, E.R., Zarina, G., Moiseyev, V., Lightfoot, E., Nigst, P.R., Manica, A., Pinhasi, R., and Bradley, D.G. (2017). The Neolithic transition in the Baltic was not driven by admixture with Early European farmers. Curr. Biol. *27*, 576–582.
80. Korneliussen, T.S., Albrechtsen, A., and Nielsen, R. (2014). ANGSD: Analysis of Next Generation Sequencing Data. BMC Bioinformatics *15*, 356.
81. Skoglund, P., Storå, J., Götherström, A., and Jakobsson, M. (2013). Accurate sex identification of ancient human remains using DNA shotgun sequencing. J. Archaeol. Sci. *40*, 4477–4482.
82. Weissensteiner, H., Pacher, D., Kloss-Brandstätter, A., Forer, L., Specht, G., Bandelt, H.-J., Kronenberg, F., Salas, A., and Schönherr, S. (2016). HaploGrep 2: mitochondrial haplogroup classification in the era of high-throughput sequencing. Nucleic Acids Res. *44*, W58–W63.
83. Quinlan, A.R. (2014). BEDTools: the Swiss-Army tool for genome feature analysis. Curr. Protoc. Bioinformatics *47*, 11.12.1–11.12.34.
84. Purcell, S., Neale, B., Todd-Brown, K., Thomas, L., Ferreira, M.A.R., Bender, D., Maller, J., Sklar, P., de Bakker, P.I.W., Daly, M.J., and Sham, P.C. (2007). PLINK: a tool set for whole-genome association and population-based linkage analyses. Am. J. Hum. Genet. *81*, 559–575.
85. Danecek, P., Auton, A., Abecasis, G., Albers, C.A., Banks, E., DePristo, M.A., Handsaker, R.E., Lunter, G., Marth, G.T., Sherry, S.T., et al.; 1000 Genomes Project Analysis Group (2011). The variant call format and VCFtools. Bioinformatics *27*, 2156–2158.
86. Browning, B.L., and Browning, S.R. (2016). Genotype imputation with millions of reference samples. Am. J. Hum. Genet. *98*, 116–126.
87. R Development Core Team (2013). R: A language and environment for statistical computing (R Foundation for Statistical Computing).
88. Link, V., Kousathanas, A., Veeramah, K., Sell, C., Scheu, A., and Wegmann, D. (2017). ATLAS: analysis tools for low-depth and ancient samples. bioRxiv. https://doi.org/10.1101/105346.

89. Chaitanya, L., Breslin, K., Zuñiga, S., Wirken, L., Pośpiech, E., Kukla-Bartoszek, M., Sijen, T., Knijff, P., Liu, F., Branicki, W., et al. (2018). The HIrisPlex-S system for eye, hair and skin colour prediction from DNA: introduction and forensic developmental validation. Forensic Sci. Int. Genet. *35*, 123–135.

90. Walsh, S., Liu, F., Wollstein, A., Kovatsi, L., Ralf, A., Kosiniak-Kamysz, A., Branicki, W., and Kayser, M. (2013). The HIrisPlex system for simultaneous prediction of hair and eye colour from DNA. Forensic Sci. Int. Genet. *7*, 98–115.

91. Fedele, F. (2013). I Covoloni del Broion (colli Berici, VI). In L'età del Rame. La pianura Padana e le Alpi al tempo di Ötzi., R. De Marinis, ed. (Compagnia della Stampa), pp. 450–456.

92. Alessandri, L., and Rolfo, M.F. (2016). L'utilizzo delle cavità naturali nella media età del Bronzo: nuovi dati dal Lazio meridionale.*CVII* (Bollettino della Unione Storia ed Arte), pp. 109–126.

93. Anzidei, A.P., and Carboni, G. (2013). L'eneolitico recente e finale nel Lazio centro-meridionale: una puntualizzazione sullo sviluppo e la durata di alcuni aspetti culturali sulla base delle più recenti datazioni radiometriche. In Cronologia Assoluta e Relativa Dell'età Del Rame in Italia, C. Genick, ed. (QuiEdit), pp. 98–118.

94. Alessandri, L. (2019). The early and Middle Bronze Age (1/2) in South and central Tyrrhenian Italy and their connections with the Avellino eruption: An overview. Quat. Int. *499*, 161–185.

95. Alessandri, L., Baiocchi, V., Del Pizzo, S., Rolfo, M.F., and Troisi, S. (2019). Photogrammetric survey with fisheye lens for the characterization of the La Sassa cave. Int. Arch. Photogramm. Remote Sens. Spatial Inf. Sci. *42-2/W9*, 25–32.

96. Anzidei, A.P., and Carboni, G. (2006). Rinaldone e Gaudo in un territorio di confine: il Lazio centro-meridionale. In Atti Del VII Incontro Di Studi Preistoria e Protostoria in Etruria. Pastori e Guerrieri Nell'Etruria Del IV e III Millennio a.C. La Civiltá Di Rinaldone a 100 Anni Dalle Prime Scoperte, N. Catacchio, ed. (Centro Studi di Preistoria e Archeologia), pp. 174–192.

97. Lovejoy, C.O. (1985). Dental wear in the Libben population: its functional pattern and role in the determination of adult skeletal age at death. Am. J. Phys. Anthropol. *68*, 47–56.

98. Rogers, T.L. (2005). Determining the sex of human remains through cranial morphology. J. Forensic Sci. *50*, 493–500.

99. Talamo, S., and Richards, M. (2011). A comparison of bone pretreatment methods for AMS dating of samples > 30,000 BP. Radiocarbon *53*, 443–449.

100. Longin, R. (1971). New method of collagen extraction for radiocarbon dating. Nature *230*, 241–242.

101. Brown, T., Nelson, D., Vogel, J., and Southon, J. (1988). Improved collagen extraction by modified Longin method. Radiocarbon *30*, 171–177.

102. Brock, F., Ramsey, C., and Higham, T. (2007). Quality assurance of ultrafiltered bone dating. Radiocarbon *49*, 187–192.

103. van Klinken, G.J. (1999). Bone collagen quality indicators for palaeodietary and radiocarbon measurements. J. Archaeol. Sci. *26*, 687–695.

104. Kromer, B., Lindauer, S., Synal, H.-A., and Wacker, L. (2013). MAMS – a new AMS facility at the Curt-Engelhorn-Centre for Achaeometry, Mannheim, Germany. Nucl. Instrum. Methods Phys. Res. B *294*, 11–13.

105. Korlević, P., Talamo, S., and Meyer, M. (2018). A combined method for DNA analysis and radiocarbon dating from a single sample. Sci. Rep. *8*, 4127.

106. Angle, M., Catracchia, F., Cavazzuti, C., Celletti, P., Malorgio, M., and Mancini, D. (2010). La grotta Regina Margherita a Collepardo (Frosinone). In Lazio e Sabina. Atti del Convegno: Sesto incontro di studi sul Lazio e la Sabina, G. Ghini, ed. (Atti del Convegno. Sesto Incontro di Studi sul La-zio e la Sabina), pp. 381–396.

107. Orlando, L., Ginolhac, A., Zhang, G., Froese, D., Albrechtsen, A., Stiller, M., Schubert, M., Cappellini, E., Petersen, B., Moltke, I., et al. (2013). Recalibrating Equus evolution using the genome sequence of an early Middle Pleistocene horse. Nature *499*, 74–78.

108. Malaspinas, A.-S., Lao, O., Schroeder, H., Rasmussen, M., Raghavan, M., Moltke, I., Campos, P.F., Sagredo, F.S., Rasmussen, S., Gonçalves, V.F., et al. (2014). Two ancient human genomes reveal Polynesian ancestry among the indigenous Botocudos of Brazil. Curr. Biol. *24*, R1035–R1037.

109. McKenna, A., Hanna, M., Banks, E., Sivachenko, A., Cibulskis, K., Kernytsky, A., Garimella, K., Altshuler, D., Gabriel, S., Daly, M., and DePristo, M.A. (2010). The Genome Analysis Toolkit: a MapReduce framework for analyzing next-generation DNA sequencing data. Genome Res. *20*, 1297–1303.

110. van Oven, M., and Kayser, M. (2009). Updated comprehensive phylogenetic tree of global human mitochondrial DNA variation. Hum. Mutat. *30*, E386–E394.

111. Hallast, P., Batini, C., Zadik, D., Maisano Delser, P., Wetton, J.H., Arroyo-Pardo, E., Cavalleri, G.L., de Knijff, P., Destro Bisol, G., Dupuy, B.M., et al. (2015). The Y-chromosome tree bursts into leaf: 13,000 high-confidence SNPs covering the majority of known clades. Mol. Biol. Evol. *32*, 661–673.

112. Karmin, M., Saag, L., Vicente, M., Wilson Sayres, M.A., Järve, M., Talas, U.G., Rootsi, S., Ilumäe, A.-M., Mägi, R., Mitt, M., et al. (2015). A recent bottleneck of Y chromosome diversity coincides with a global change in culture. Genome Res. *25*, 459–466.

113. Poznik, G.D., Xue, Y., Mendez, F.L., Willems, T.F., Massaia, A., Wilson Sayres, M.A., Ayub, Q., McCarthy, S.A., Narechania, A., Kashin, S., et al.; 1000 Genomes Project Consortium (2016). Punctuated bursts in human male demography inferred from 1,244 worldwide Y-chromosome sequences. Nat. Genet. *48*, 593–599.

114. Broushaki, F., Thomas, M.G., Link, V., López, S., van Dorp, L., Kirsanow, K., Hofmanová, Z., Diekmann, Y., Cassidy, L.M., Díez-Del-Molino, D., et al. (2016). Early Neolithic genomes from the eastern Fertile Crescent. Science *353*, 499–503.

115. Harney, É., May, H., Shalem, D., Rohland, N., Mallick, S., Lazaridis, I., Sarig, R., Stewardson, K., Nordenfelt, S., Patterson, N., et al. (2018). Ancient DNA from Chalcolithic Israel reveals the role of population mixture in cultural transformation. Nat. Commun. *9*, 3336.

116. Günther, T., Malmström, H., Svensson, E.M., Omrak, A., Sánchez-Quinto, F., Kılınç, G.M., Krzewińska, M., Eriksson, G., Fraser, M., Edlund, H., et al. (2018). Population genomics of Mesolithic Scandinavia: Investigating early postglacial migration routes and high-latitude adaptation. PLoS Biol. *16*, e2003703.

117. Mittnik, A., Wang, C.-C., Pfrengle, S., Daubaras, M., Zariņa, G., Hallgren, F., Allmäe, R., Khartanovich, V., Moiseyev, V., Tõrv, M., et al. (2018). The genetic prehistory of the Baltic Sea region. Nat. Commun. *9*, 442.

118. van den Brink, E.C.M., Beeri, R., Kirzner, D., Bron, E., Cohen-Weinberger, A., Kamaisky, E., Gonen, T., Gershuny, L., Nagar, Y., Ben-Tor, D., et al. (2017). A Late Bronze Age II clay coffin from Tel Shaddud in the Central Jezreel Valley, Israel: context and historical implications. Levant *49*, 105–135.

119. Valdiosera, C., Günther, T., Vera-Rodríguez, J.C., Ureña, I., Iriarte, E., Rodríguez-Varela, R., Simões, L.G., Martínez-Sánchez, R.M., Svensson, E.M., Malmström, H., et al. (2018). Four millennia of Iberian biomolecular prehistory illustrate the impact of prehistoric migrations at the far end of Eurasia. Proc. Natl. Acad. Sci. USA *115*, 3428–3433.

120. Fregel, R., Méndez, F.L., Bokbot, Y., Martín-Socas, D., Camalich-Massieu, M.D., Santana, J., Morales, J., Ávila-Arcos, M.C., Underhill, P.A., Shapiro, B., et al. (2018). Ancient genomes from North Africa evidence prehistoric migrations to the Maghreb from both the Levant and Europe. Proc. Natl. Acad. Sci. USA *115*, 6774–6779.

121. Jones, E.R., Gonzalez-Fortes, G., Connell, S., Siska, V., Eriksson, A., Martiniano, R., et al. (2015). Upper Palaeolithic genomes reveal deep roots of modern Eurasians. Nat. Commun. *6*.

122. Patterson, N., Moorjani, P., Luo, Y., Mallick, S., Rohland, N., Zhan, Y., Genschoreck, T., Webster, T., and Reich, D. (2012). Ancient admixture in human history. Genetics *192*, 1065–1093.

123. Busby, G.B.J., Hellenthal, G., Montinaro, F., Tofanelli, S., Bulayeva, K., Rudan, I., et al. (2015). The role of recent admixture in forming the contemporary West Eurasian genomic landscape. Curr. Biol. *25*, 2878–2526.

124. Browning, S.R., Browning, B.L., Zhou, Y., Tucci, S., and Akey, J.M. (2018). Analysis of human sequence data reveals two pulses of archaic Denisovan admixture. Cell *173*, 53–61.e9.

125. Gamba, C., Jones, E.R., Teasdale, M.D., McLaughlin, R.L., Gonzalez-Fortes, G., Mattiangeli, V., Domboróczki, L., Kővári, I., Pap, I., Anders, A., et al. (2014). Genome flux and stasis in a five millennium transect of European prehistory. Nat. Commun. *5*, 5257.

126. Narasimhan, V., Danecek, P., Scally, A., Xue, Y., Tyler-Smith, C., and Durbin, R. (2016). BCFtools/RoH: a hidden Markov model approach for detecting autozygosity from next-generation sequencing data. Bioinformatics *32*, 1749–1751.

STAR★METHODS

KEY RESOURCES TABLE

REAGENT or RESOURCE	SOURCE	IDENTIFIER
Biological samples		
Ancient skeletal element	This paper	BRC001
Ancient skeletal element	This paper	BRC002
Ancient skeletal element	This paper	BRC003
Ancient skeletal element	This paper	BRC007
Ancient skeletal element	This paper	BRC010
Ancient skeletal element	This paper	BRC011
Ancient skeletal element	This paper	BRC013
Ancient skeletal element	This paper	BRC015
Ancient skeletal element	This paper	BRC022
Ancient skeletal element	This paper	BRC024
Ancient skeletal element	This paper	BRC030
Ancient skeletal element	This paper	GCP002
Ancient skeletal element	This paper	GCP003
Ancient skeletal element	This paper	GCP004
Ancient skeletal element	This paper	GLR001
Ancient skeletal element	This paper	GLR002
Ancient skeletal element	This paper	GLR003
Ancient skeletal element	This paper	GLR004
Ancient skeletal element	This paper	LSC002
Ancient skeletal element	This paper	LSC005
Ancient skeletal element	This paper	LSC007
Ancient skeletal element	This paper	LSC011
Chemicals, peptides, and recombinant proteins		
Sodium Hypochlorite solution (15%)	N/A	CAS:7681-52-9
0.5 M EDTA pH 8.0	Fisher Scientific	Cat# BP24821
Ethanol 96%	Chemlab	Cat# CL00.0507.1000
dNTP Mix (25mM each)	Thermo Fisher Scientific	Cat# R1122
dNTP Mix (10mM each)	Thermo Fisher Scientific	Cat# R0192
BSA	Thermo Fisher Scientific	Cat# B14
HGS Diamond Taq	Eurogentec	Cat# TAQ-I011-5000+
Critical commercial assays		
MinElute PCR Purification Kit	QIAGEN	Cat# 28006
High Pure Viral Nucleic Acid LargeVolume Kit	Roche	Cat# 5114403001
NEBNext DNA Library Prep Master Mix Set 454	New England Biolabs	Cat# E6070L
Qubit dsDNA BR Assay Kit	Thermo Fisher Scientific	Cat# Q32853
Qubit dsDNA HS Assay Kit	Thermo Fisher Scientific	Cat# Q32854
Fragment Analyzer High Sensitivity NGS Fragment Analysis Kit	Agilent	Cat# DNF-474-0500
D1000 ScreenTape	Agilent	Cat# 5067-5582
D1000 Reagents	Agilent	Cat# 5067-5583
High Sensitivity D1000 ScreenTape	Agilent	Cat# 5067-5584

(*Continued on next page*)

Continued

REAGENT or RESOURCE	SOURCE	IDENTIFIER
High Sensitivity D1000 Reagents	Agilent	Cat# 5067-5585
KAPA Library Quantification Kit	Roche	Cat# KK4835
Deposited data		
Human reference genome NCBI build 37, GRCh37	Genome Reference Consortium	https://www.ncbi.nlm.nih.gov/projects/genome/assembly/grc/human/
Mitochondrial DNA reference genome, cRSRS	Behar et al.[71]	https://www.ncbi.nlm.nih.gov/pmc/articles/PMC3322232/#!po=70.8333
Compiled modern and ancient comparison dataset (including restricted access samples) 1240K and Human Origins	N/A	https://reichdata.hms.harvard.edu/pub/datasets/amh_repo/curated_releases/index_v42.4.html
1000 Genomes Project Phase 3	The 1000 Genomes Project Consortium[62]	https://www.internationalgenome.org/category/phase-3/
Haplotype Reference Consortium	McCarthy et al.[72]	http://www.haplotype-reference-consortium.org/
Italian aDNA data	This paper	http://www.ebc.ee/free_data; http://www.ebi.ac.uk/ena/data/view/PRJEB37660; ENA: PRJEB37660
Oligonucleotides		
NEBNext Multiplex Oligos for Illumina	New England Biolabs	Cat# E7335
IS1_adapter.P5 A*C*A*C*TCTTTCCCTACACG ACGCTCTTCCG*A*T*C*T	Meyer and Kircher[73]	Eurofins
IS2_adapter.P7 G*T*G*A*CTGGAGTTCAGACGTG TGCTCTTCCG*A*T*C*T	Meyer and Kircher[73]	Eurofins
IS3_adapter.P5+P7 A*G*A*T*CG GAA*G*A*G*C	Meyer and Kircher[73]	Eurofins
Software and algorithms		
cutadapt	Martin[74]	https://cutadapt.readthedocs.io/en/stable/#
Burrow-Wheeler Aligner (BWA 0.7.12)	Li and Durbin[75]	http://bio-bwa.sourceforge.net/
Samtools 1.3, 1.6, 1.9	Li et al.[76]	http://samtools.sourceforge.net/
Picard 2.12, 1.54	N/A	http://broadinstitute.github.io/picard/
GATK 3.5	DePristo et al.[77]	https://gatk.broadinstitute.org
mapDamage 2.0	Jónsson et al.[78]	https://ginolhac.github.io/mapDamage/
mtDNA contamination algorithm	Jones et al.[79]	N/A
ANGSD-0.916	Korneliussen et al.[80]	http://www.popgen.dk/angsd/index.php/ANGSD
sex determination algorithm #1	Skoglund et al.[81]	https://github.com/pontussk/ry_compute
sex determination algorithm #2	Fu et al.[15]	N/A
HaploGrep2	Weissensteiner et al.[82]	https://haplogrep.i-med.ac.at/category/haplogrep2/
BEDTools	Quinlan[83]	https://bedtools.readthedocs.io/en/latest/
PLINK v1.90b3.27	Purcell et al.[84]	https://www.partners.org/purcell/plink/
EIGENSOFT 7.2.0	Patterson et al.[44]	https://github.com/DReichLab/EIG
ADMIXTOOLS	Price et al.[45]	https://github.com/DReichLab/AdmixTools
ADMIXTURE	Alexander et al.[53]	https://bio.tools/admixture
ChromoPainter/NNLS pipeline	Lawson et al.[55]	https://people.maths.bris.ac.uk/~madjl/finestructure-old/chromopainter_info.html
SourceFind	Chacón-Duque et al.[56]	https://people.maths.bris.ac.uk/~madjl/finestructure/sourcefind.html

(*Continued on next page*)

Continued

REAGENT or RESOURCE	SOURCE	IDENTIFIER
READ	Monroy Kuhn et al.[40]	https://bitbucket.org/tguenther/read
VCFtools	Danecek et al.[85]	http://vcftools.sourceforge.net/
Datagraph	MacAskill[63]	https://visualdatatools.com/
Beagle 4.1, 5.0	Browning and Browning[86]	https://faculty.washington.edu/browning/beagle/b4_1.html
R 3.6	R Development Core Team[87]	http://www.R-project.org/
ATLAS v0.9.0	Link et al.[88]	https://bitbucket.org/wegmannlab/atlas/wiki/Home
hapROH	Ringbauer et al.[61]	https://pypi.org/project/hapROH/
HIrisPlex-S	Chaitanya et al.[89] and Walsh et al.[90]	https://hirisplex.erasmusmc.nl/

RESOURCE AVAILABILITY

Lead contact

Further information and requests for resources and reagents should be directed to and will be fulfilled by the Lead Contact: Tina Saupe (tina.saupe@ut.ee).

Materials availability

This study did not generate new unique reagents.

Data and code availability

The accession number for the DNA sequences reported in this paper is ENA:PRJEB37660 (https://www.ebi.ac.uk/ena/data/view/PRJEB37660). The data are also available through the data depository of the EBC (http://evolbio.ut.ee).

EXPERIMENTAL MODEL AND SUBJECT DETAILS

The DNA was extracted from 47 bone and tooth samples in 51 extracts, 51 double-stranded, single-indexed libraries generated: 30 from Grottina dei Covoloni del Broion, 13 from Grotta La Sassa, four from the Necropoli di Gattolino di Cesena and four from Grotta Regina Margherita. Forty-nine libraries were NGS screened at low depth and 20 sequenced to higher coverage and analyzed. More detailed information about the archaeological sites of this study are given below.

Grottina dei Covoloni del Broion

Tina Saupe & Cinzia Scaggion

The Grottina dei Covoloni del Broion is part of the oriental rocky wall complex of Colli Berici. It is close to the famous cave Grotta Broion in the province of Vicenza in Northern Italy where among Paleolithic sediments, the Italian geologist Piero Leonardi found significant traces of Neanderthal. This prehistoric shelter is located in Vallà di Lumignano in the municipality of Longare and was used as a funerary site. Through the analysis of the palaeosurface, the site seems to have been used for a long time covering many generations belonging to the Chalcolithic confirmed by the discovery of Eneolithic artifacts.

Grottina dei Covoloni del Broion was discovered in 1973 and systematic excavations were conducted of the different geological layers and of parts of the Grottina during four archeological campaigns between 1973 and 1977. The archaeological excavation of 1977 was entirely reserved for the study of funerary depositions. The inner part of the cave was intended for sepulchral use such as was evidenced by the discovery of many human osteological findings incorporated in the calcareous sediment. The archaeologists had also found ceramic fragments and many flint artifacts: a flat blade of dagger, a significant amount of arrow cusps, blades, two flint cores, small discoid beads and a small calcite tube from a bracelet or necklace, and other personal ornaments found in the same layer. The human remains include bones and teeth under different states of conservation and distribution.[91] For this study, in collaboration with the University of Padova and Museum of Anthropology of Padova, samples of 26 human remains (pars petrous bone = 4, teeth = 22) were taken with unknown morphological background of age and sex. Samples BRC001, BRC002, BRC003, BRC007, BRC010, BRC013, BRC022, and BRC030 were dated at ^{14}CHRONO Centre for Climate, the Environment, and Chronology in Belfast, UK (Data S1C).

Grotta La Sassa

Luca Alessandri, Ilenia Arienzo, Flavio De Angelis and Mario Federico Rolfo

The Grotta La Sassa (National Cave Cadastre id: LA 2001) was discovered in 2015 during a survey of the Ausoni Mountains natural caves carried out by two speleological groups: Gruppo Grotte Castelli Romani and Speleo Club Roma.[92] Several archaeological surveys have been carried out in the cave, from 2016 to the present day by the Groningen Institute of Archaeology and the University of

Rome Tor Vergata. The cave is in the valley close to the modern town of Sonnino (Latina, Italy). The coordinates of the entrance are: WGS84, UTM 33T, 352627E, 4587452N. The cave yields an impressive stratigraphy ranging from the late Pleistocene to the Second World War, when the cave was used as a hiding shelter by the locals. Hundreds of disarticulated human bones and teeth scattered in Room 1 (soundings N, WD and L) and Room 2 were collected (Figure S1A). They have been radiocarbon dated to the Copper Age and the Early Bronze Age (for the Italian chronology, see Anzidei and Carboni[93] and Alessandri[94]). The sampled bones pertaining to this work come from the stratigraphic units (SUs) 19, 31 and 36, in Room 2 (Figure S1B).

The three radiocarbon dates that come from human bones in SU 19 set the layer in the Copper Age/Chalcolithic. SUs 31 and 36 belong to a group of layers which contain Middle Bronze Age potsherds, possibly reworked in Medieval times (Figure S1). However, the four radiocarbon dates which have been obtained from these samples are all tightly clustered around 4,050 BP (Figure S1D) which, in Italian chronology, falls into the Late Copper Age. No pottery items were found in association with these bones, despite the only Copper Age potsherds collected in the cave (Figure 13 in Alessandri et al.[95]) belonging to the Gaudo funeral facies,[96] which is characteristic of Southern Italy.

The anthropological samples were recruited for micro-sampling at the University of Rome "Tor Vergata" and the sampling process was performed at Oxford University afterward. The visual preservation status was the driving inclusion criterion for the recruitment.

The osteological characteristics of the selected bones suggested that the fragments could belong to different individuals, even though the molecular analyses later showed that the bone fragments pertaining to LSC002 and LSC004 come from the same individual. These bone fragments consist of diagenetically damaged petrous bones and their siding are not reliably assessed by morphological evaluation.

LSC005 is a lower second molar tooth pertaining to an adult individual, whose age at death could be set as 35-40 years old according to classical osteological methods.[97]

LSC007 is an upper first molar related to a young adult whose age at death should be between 15 and 20 years old according to the lack of enamel wear.[97]

LSC011 refers to a lower first molar dental element carried by a mandible of an adult male individual whose age at death should be set up to 40 years old.[97,98]

The samples are already submitted to multi-isotope analysis for unravelling diet and mobility of people buried in Grotta La Sassa. The mobility of the ancient people buried in La Sassa is currently under evaluation and the data will be conclusive shortly with the publication of a dedicated paper in preparation. For the purpose of the present paper, the punctual data pertaining to the sampled teeth are reported. Remarkably, LSC005 returns an enamel 87Sr/86Sr ratio of 0.709549, which is out of the range determined for the rest of 27 sampled teeth from the cave. The LSC011 and LSC007 samples return an enamel 87Sr/86Sr ratio of 0.709308 and 0.708800, respectively, that are tuned with the data recovered from the rest of the teeth in La Sassa.

Samples LSC002/004, LSS005/013 and LSC011 were dated at ^{14}CHRONO Centre for Climate, the Environment, and Chronology in Belfast, UK (Data S1C).

Necropoli di Gattolino di Cesena

Monica Miari

The Necropoli of Gattolino is located in the municipality of Cesena (Emilia-Romagna region, central Italy). The four graves were probably part of a larger Copper Age necropolis. The graves were all single, NW-SE oriented and the inhumations were in a lying supine position. The burials included a vessel placed at the foot of the body in addition to flint artifacts, in particular arrow-heads. Based on the materials, the necropolis highlights important contacts with central and southern Italy - with particular regard to the Laterza *facies* - and seems to be framed from a recent phase of the Copper Age to the beginning of the Bronze Age, due to the presence in the Grave 1 of beads in Sicilian amber and silver.

Radiocarbon method and date of Gattolino

Sahra Talamo

The Gattolino bone collagen was extracted at the Department of Human Evolution, Max Planck Institute for Evolutionary Anthropology (MPI-EVA) in Leipzig, Germany, following the pretreatment procedures in Talamo and Richards[99] (MPI-Code: S-EVA). The outer surface of the bone sample is first cleaned by a shot blaster and then 500 mg of the whole bone is taken. The samples are then decalcified in 0.5M HCl at room temperature until no CO_2 effervescence is observed. 0.1M NaOH is added for 30 minutes to remove humics. The NaOH step is followed by a final 0.5M HCl step for 15 minutes. The resulting solid is gelatinized following Longin[100] at pH 3 in a heater block at 75°C for 20h. The gelatine is then filtered in an Eeze-Filter (Elkay Laboratory Products (UK)) to remove small (> 80 mm) particles. The gelatine is then ultrafiltered[101] with Sartorius "VivaspinTurbo" 30 KDa ultrafilters. Prior to use, the filter is cleaned to remove carbon containing humectants.[102] The samples are lyophilized for 48 hours. C:N atomic ratios, and collagen yields were measured to determine the extent of collagen preservation. Bones with > 1% weight collagen and C:N ratios in the range 2.9–3.6 are passing the evaluation criteria for collagen to proceed with the AMS analysis.[103] Samples were graphitised and dated by AMS at the Mannheim facility (laboratory code MAMS[104]).

In order to monitor contamination introduced during the pretreatment stage, a sample from a cave bear bone, kindly provided by D. Döppes (MAMS, Germany), was extracted along with the batch of La Ferrassie samples.[105] The Gattolino collagen sample passed the evaluation criteria for good quality collagen and is reported in Data S1C. The Radiocarbon date of Gattolino 3 was calibrated using IntCal20;[41] with the OxCal 4.4 program.[43] The C:N ratio and the amount of collagen extracted (%Coll, > 30 kDa fraction) are reported.

Grotta Regina Margherita

Robin Skeates

Grotta Regina Margherita is situated in the modern municipality of Collepardo (Frosinone province, Westcentral Italy). It is a large limestone karst cave. It is located at an altitude of 480 m in the Fiume valley, and opens about 30 m above the bottom of a gorge and below the hill on which the Medieval village of Collepardo now sits. It is the largest known mortuary cave in Middle Bronze Age Central Italy (c. 1650-1400 BCE). Essentially, the cave can be divided into two contrasting zones: the twilight Entrance Hall and the dark Interior Hall. Since 2008,[106] our team has excavated and compared soundings in the archaeological deposits found in diverse areas of the cave. The three aDNA samples of human petrous bone come from two different soundings in the Interior Hall. In this part of the cave, we found clear evidence for primary and secondary mortuary rites having been performed in the Middle Bronze Age in well-defined spaces enclosed by speleothems- distinguished archaeologically by concentrations of human remains and body ornaments. This mortuary activity in the cave has been radiocarbon dated to between c. 1650 and 1450 cal BC.

Sample B297 comes from Sounding D, Context 32

Sounding D lies in a relatively well-defined sunken space delimited by large speleothems. Here, a rich and relatively extensive mortuary deposit has been identified, comprising a dense and compact 'carpet' of human bones and associated artifacts (Context 32), embedded in a fine cave loam and patches of calcite crust. Finds include: human and animal bones, pottery fragments, a clay spindle whorl, two fragments of a small bronze ornament made of a cylindrical spiral of wire to which is attached a fragment of a faïence bead, a disc-shaped bead or button of mother-of-pearl, a quadrangular piece of sandstone, with wear traces from use in sharpening or smoothing, and some pieces of charcoal. The human remains recovered so far (from the upper two thirds of the deposit) belong to at least 19 individuals, with ten adults (including at least three young adults and one older adult of 40-60 years) and 9 sub-adults (one fetus/perinatal individual, one infant of 18 months, one infant of approximately 2 years, one child of approximately 3-6 years, one child of approximately 8 years, one older child of 10 years, and three adolescents). There are at least two females and one male adult. Despite the generally disarticulated (and also somewhat fragmented) state of the human remains, a few of the bones (including some phalanges) were found in articulation, and all bones from the skeleton (including many small and fragile bones) were represented, suggesting the original deposition of whole bodies in this area. However, the significant under-representation of long bones (particularly the lower limbs-tibiae and femurs) hints at the successive removal of large bones from this area, which might then have been redeposited elsewhere in or beyond the cave. The presence of mineralised breaks and calcite accretions covering breakage points also indicates that most of the bones were fragmented prior to the formation of the calcite, quite possibly unintentionally in the Bronze Age during the course of primary and secondary mortuary rites, which added to and disturbed earlier mortuary deposits in this area.

We obtained 10 radiocarbon determinations on human bones from Sounding D, to gain some idea of the period of time over which these mortuary deposits were formed, selecting only left heels (astragali) to ensure that we were dating different individuals. The basic time span provided by these determinations, at the 68 per cent probability level, is c. 1600-1450 cal BCE. Using Bayesian chronological modeling, at the same probability level, the period of activity can be narrowed down to 1-60 years, falling within 1545-1480 cal BCE.

Samples B152 and B154 come from Sounding E, Context 60

Sounding E comprises a small sunken space situated among a group of speleothems. It is the innermost area excavated in the cave. The deposits in this area are loose, having been heavily disturbed by the installation of the tourist walkway. Context 60 is the uppermost layer of these deposits. Numerous concrete human bones, a few pottery fragments, and some charcoal and ashes were found here. A minimum number of 7 individuals is represented by the human bones, with three adults and four sub-adults (one infant of less than one year, one child of around 6 years, one child of around 9 years, and one adolescent). There is at least one female adult and one male adult. Exceptionally, a humerus and an ulna were found in anatomical connection here. This, together with the relatively high average frequency of representation of skeletal elements in this area (50 per cent), indicates the successive primary deposition of whole bodies in this area.

A human left astragalus (SUERC-78150) from Sounding E has a radiocarbon date of c. 1500–1450 cal BC, which is contemporary with some of the dated left astragali from Sounding D.

Samples GCP002 and GCP003 were dated at ^{14}CHRONO Centre for Climate, the Environment, and Chronology in Belfast, UK (Data S1C).

METHOD DETAILS

All of the laboratory work was performed in dedicated ancient DNA laboratories at the Estonian Biocenter, Institute of Genomics, University of Tartu, Tartu, Estonia. The library quantification and sequencing were performed at the Estonian Biocenter Core Laboratory. The main steps of the laboratory work are detailed below.

DNA extraction

In total 47 samples from human remains were extracted for DNA analysis. The four petrous bones from Broion cave were sampled twice, giving a total of 51 extracts.

The first layer of pars petrous was removed with a sterilized drill bite to avoid exogenous contamination. Bone powder and a 10 mm core of the inner ear were sampled from the pars petrous. The drill bits and core drill were sterilized in between samples with 6% (w/v) bleach followed by distilled water and then ethanol rinse. Root portions of teeth were removed with a sterile drill wheel.

The root and the petrous portions were soaked in 6% (w/v) bleach for 5 minutes. Samples were rinsed three times with 18.2 MΩcm H_2O and soaked in 70% (v/v) Ethanol for 2 minutes. The tubes were shaken during the procedure to dislodge particles. The samples were transferred to a clean paper towel on a rack inside a class IIB hood with the UV light on and allowed to dry for two to three hours.

Afterward, the samples were weighed to calculate the accurate volume of EDTA (20x EDTA [μl] of sample mass [mg]) and Proteinase K (0.5x Proteinase K [μl] of sample mass [mg]). EDTA and Proteinase K were added into PCR-clean 5 mL or 15 mL conical tubes (Eppendorf) along with the samples inside the IIB hood and the tubes were incubated 72 h on a slow shaker at room temperature. 1000 μl of EDTA and 25 μl of Proteinase K were added to the bone powder of the pars petrous and were incubated 24 h on a slow shaker at room temperature.

The DNA extracts (of root portions, pars petrous portions and bone powder) were concentrated to 250 μl using the Vivaspin Turbo 15 (Sartorius) and purified in large volume columns (High Pure Viral Nucleic Acid Large Volume Kit, Roche) using 2.5 mL of PB buffer, 1 mL of PE buffer and 100 μL of EB buffer (MinElute PCR Purification Kit, QIAGEN). For the elution of the endogenous DNA, the silica columns were transferred to a collection tube to dry and followed in 1.5 mL DNA lo-bind tubes (Eppendorf) to elute. The samples were incubated with 100 μl EB buffer at 37 C for 10 minutes and centrifuged at 13,000 rpm for two minutes. After centrifugation, the silica columns were removed and the samples were stored at −20 C. Only one extraction was performed per extraction for screening and 30 μl used for libraries.

Library preparation

Sequencing libraries were built using NEBNext DNA Library Prep Master Mix Set for 454 (E6070, New England Biolabs) and Illumina-specific adaptors[73] following established protocols.[73,107,108] The end repair module was implemented using 18.75 μL of water, 7.5 μL of buffer and 3.75 μL of enzyme mix, incubating at 20°C for 30 minutes. The samples were purified using 500 μL PB and 650 μL of PE buffer and eluted in 30 μL EB buffer (MinElute PCR Purification Kit, QIAGEN). The adaptor ligation module was implemented using 10 μL of buffer, 5 μL of T4 ligase and 5 μL of adaptor mix,[73] incubating at 20°C for 15 minutes. The samples were purified as in the previous step and eluted in 30 μL of EB buffer (MinElute PCR Purification Kit, QIAGEN). The adaptor fill-in module was implemented using 13 μL of water, 5 μL of buffer and 2 μL of Bst DNA polymerase, incubating at 37°C for 30 and at 80°C for 20 minutes. Libraries were amplified using the following PCR set up: 50 μL DNA library, 1X PCR buffer, 2.5mM MgCl2, 1 mg/ml BSA, 0.2 μM inPE1.0, 0.2mM dNTP each, 0.1U/μl HGS Taq Diamond and 0.2 μM indexing primer. Cycling conditions were: 5′ at 94C, followed by 18 cycles of 30 s each at 94C, 60C, and 68C, with a final extension of 7 minutes at 72C. The samples were purified and eluted in 35 μL of EB buffer (MinElute PCR Purification Kit, QIAGEN). Three verification steps were implemented to make sure library preparation was successful and to measure the concentration of dsDNA/sequencing libraries - fluorometric quantitation (Qubit, Thermo Fisher Scientific), parallel capillary electrophoresis (Fragment Analyzer, Agilent Technologies) and qPCR.

DNA sequencing

DNA was sequenced using the Illumina NextSeq500/550 High-Output single-end 75 cycle kit. As a norm, 15 samples were sequenced together on one flow cell; additional data was generated for 20 samples to increase coverage (Data S1).

QUANTIFICATION AND STATISTICAL ANALYSIS

Mapping

Before mapping, the sequences of the adapters, indexes, and poly-G tails occurring due to the specifics of the NextSeq 500 technology were cut from the ends of DNA sequences using cutadapt-1.11.[74] Sequences shorter than 30 bp were also removed with the same program to avoid random mapping of sequences from other species. The sequences were aligned to the reference sequence GRCh37 (hs37d5) using Burrows- Wheeler Aligner (BWA 0.7.12)[75] and the command mem with re-seeding disabled.

After alignment, the sequences were converted to BAM format and only sequences that mapped to the human genome were kept with samtools 1.3.[76] Afterward, the data from different flow cell lanes were merged and duplicates were removed using picard 2.12 (http://broadinstitute.github.io/picard/index.html). Indels were realigned using GATK 3.5[109] and reads with a mapping quality less than 10 were filtered out using samtools 1.3.[76]

aDNA authentication

As a result of degrading over time, aDNA can be distinguished from modern DNA by certain characteristics: short fragments and a high frequency of C = > T substitutions at the 5′ ends of sequences due to cytosine deamination. The program mapDamage2.0[78] was used to estimate the frequency of 5′ C = > T transitions. Rates of contamination were estimated on mitochondrial DNA by calculating the percentage of non-consensus bases at haplogroup-defining positions as detailed in Jones et al.[79] Each sample was mapped against the RSRS downloaded from phylotree.org and checked against haplogroup-defining sites for the sample-specific haplogroup (Data S1).

Samtools 1.9[76] option *stats* was used to determine the number of final reads, average read length, average coverage etc. The average endogenous DNA content (proportion of reads mapping to the human genome) was 10.77% (0.48 - 48.87%) (Data S1A and S1B).

Calculating genetic sex estimation

Genetic sex was calculated using the methods described in Skoglund et al.,[81] estimating the fraction of reads mapping to Y chromosome out of all reads mapping to either X or Y chromosome. Additionally, sex was determined using a method described in Fu et al.,[15] calculating the X and Y ratio by the division of the coverage by the autosomal coverage. Here, the sex was calculated for samples with a coverage > 0.01 × and only reads with a mapping quality > 10 were counted for the autosomal, X, and Y chromosome (Data S1A and S1B).

Determining mtDNA haplogroups

Mitochondrial DNA haplogroups were determined using Haplogrep2 on the command line. For the determination, the reads were re-aligned to the reference sequence RSRS and the parameter -rsrs were given to estimate the haplogroups using Haplogrep2[82,110] (Data S1B). Subsequently, the identical results between the individuals were checked visually by aligning mapped reads to the reference sequence using samtools 0.1.19[76] command *tview* and confirming the haplogroup assignment in PhyloTree. Additionally, private mutations were noted for further kinship analysis (Data S1E). The polymorphisms were estimated using the online platform of haplogrep2. Here, the variant calling files (*vcf.*) were uploaded to the online platform and the known polymorphism in the RSRS were converted to rCRS (Data S1E).

Y chromosome variant calling and haplotyping

A total of 138,425 binary Y chromosome SNPs that have been detected as polymorphic in previous high coverage whole Y chromosome sequencing studies[111–113] were called in Chalcolithic/Bronze Age samples using ANGSD-0.916[80] command–doHaploCall. Only ten individual samples that had more than 0.01 × Y chromosome variant coverage were kept for further analyses. A subset of 105,691 sites yielded a call in at least one of the samples and in case of 2,480 sites at least one of the ten samples carried a derived allele. Basal haplogroup affiliations of each sample were determined by assessing the proportion of derived allele calls (pD) in a set of primary (A, B, C...T) haplogroup defining internal branches, as defined in Karmin et al.,[112] using 1,677 informative sites. In case of all ten samples the primary haplogroup could be determined unambiguously (pD > 0.85) with the support of at least 4 variants in derived state considering the pD values outside the path connecting the root of the Y chromosome tree and the respective haplogroup were observed in the range of 0-0.037. Further detailed sub-haplogroup assignments within the phylogeny of the primary haplogroup were determined on the basis of mapping the derived allele calls to the internal branches of a tree based on modern high coverage genomes and highlighting the marker tagging the branch with the lowest derived allele frequency (Data S1B and S1F).

Kinship analysis and identical samples

Preparing data for analysis

First, all newly generated samples were called with ANGSD-0.916[80] command–doHaploCall, sampling a random base for the positions that are present at MAF > 0.1 in the 1000 Genomes GBR population[62] giving a total of 4,446,224 SNPs for autosomal kinship analysis.

For the comparison with published studies, we used the 1240k panel SNPs only and select populations (Data S4) were retained from the combined dataset using plink–keep and converted to .tped. We chose two sets of contemporaneous samples (CA and BA) and only samples with > 0.1x coverage were included. The ANGSD output files were converted to .tped format, which was used as an input for kinship analyses with READ.[40]

Identifying genetically identical individuals

When using this approach the coverage, sample size and population diversity is important. Recommended minimum coverage combined between compared individuals is 0.1x[40] for accurate relationship estimation and too small a sample size will shift the estimated P0 upward leading to false negatives (not detecting 1st or 2nd degree relatives) and too much population diversity, i.e., analyzing completely different populations together (separated by too much time, distance etc.) will shift the P0 values lower, leading to false positives. Keeping this in mind, we first used the tool to identify the redundant sampling of identical individuals within sites. All samples over 0.1x were first run and any identical samples merged. Then one sample of lower than 0.1x was tested against the newly merged set starting with the highest coverage (e.g., 0.08x then 0.06x) and each time if the low coverage sample was estimated to be identical to any other sample, it was merged. If it was not, it was removed from the pool. Only if the estimated mtDNA haplotype and the READ analysis matched (showed identical) were they merged. This process was repeated until all samples with over 100,000 reads mapping to hg19 had been tested. We also checked the method using samples BRC027-29, which were powders taken from the same petrous bones as BRC001-3. The approach correctly identified the matches in these three cases. Using this approach we estimate the minimum/maximum number of individuals per site to be: Broion (12-15) and La Sassa (4-9).

Identifying kinship in new samples

Once identical individuals were identified and merged, to assess kinship relationships up to the 3rd degree, we divided the samples several ways according to geography and time. First all sites were analyzed together regardless of time period, then all sites

separated into Chalcolithic and Bronze Age based on C14 dates and genetic clustering on the PCA (EN versus PN clusters), then each site separately with Broion also run in two ways: 1) all samples together and 2) separated into Chalcolithic and Bronze Age sets. The mean P0 values are consistent across groupings (Data S4A) when assessing the results output, only pairs in which both the lower and upper Z score are greater than 4 are reported in Table 2. The full list of comparative genomes is listed in Data S4B, newly reported CA and BA results in Data S4C and S4D. Our main analysis is restricted to samples over 0.05x; however, we did run some tests on individuals over 0.0005x as part of the exploration of identical samples, these results are in Data S4E and S4F. We also compared our newly generated genomes (> 0.05x) to published CA and BA samples as listed in Data S4B, restricting analysis to published genomes over 0.1x. Results are listed in Data S4G–S4J, with no new confirmed close kinship relationships to report.

Imputed genomes (see section Genome imputation) were used to study in further detail cases of close degree of genetic relatedness detected with READ. We used the–genome function of PLINK 1.9.0[59] to estimate pairwise proportions of IBD1 and IBD2 that are informative, for example, for distinguishing parent-offspring from sibling relationships (Table 2).

Preparing the datasets for autosomal analysis

For the chronological sample assignment for the study of the arrival of Steppe-related ancestry component in Italy, comparative ancient samples from the Italian Peninsula, Sardinia, and Sicily broadly dated from the Neolithic to the Iron Age were added to the dataset along with the newly generated ancient samples from this study.[7,9,13,14,16,17] We used the following ranges for the time periods: Neolithic ((N), 7000 - 3500 BCE), Copper Age/Chalcolithic ((CA), 3500 - 2200 BCE), Early Bronze Age ((EBA), 2200 - 1700 BCE), Bronze Age ((BA), 1700 - 900 BCE), and Iron Age ((IA), 900 - 200 BCE) and grouped samples using the published relative and absolute dates. Because of the different chronological association of the transition from the Copper Age to the Bronze Age in Sardinia, ancient samples from the Nuragic culture were grouped with other ancient samples from Sardinia dated to the Bronze Age and ancient samples from the Punic culture were grouped with samples dated to the Iron Age (see also Data S1D).

20 individuals were sequenced in additional runs to an average genomic coverage between 0.13 and 1.24x. Sequences were re-aligned using the same process as previously described and identical individuals were merged using samtools 1.6[76] command *merge* and duplicates were removed using picard tools 1.54 (http://broadinstitute.github.io/picard/index.html).

In total, 22 individuals were selected for genomic analysis (Table 1; Data S1). Autosomal variants were called with ANGSD-0.916[80] command–doHaploCall calling all the positions in the Lazaridis et al., 2016 aDNA dataset.[46] For the analysis, a dataset of ancient and present-day individuals from David Reich Lab (https://reich.hms.harvard.edu/allen-ancient-dna-resource-aadr-downloadable-genotypes-present-day-and-ancient-dna-data, release: 1st of March 2020) and the dataset from Fernandes et al.[16] and Marcus et al.[17] were merged using PLINK v1.90[59] (Table S4). We performed all subsequent analysis on autosomal data. However, we excluded published ancient samples from Sardinia and Sicily which had been annotated as low coverage or contaminated samples and *group_label_sampleID*.

We created two different datasets maximizing SNP coverage in 1) *modern* (1240K +HO) and 2) *ancient* samples (1240K). The *modern* dataset was used to perform principal component analysis, DyStruct, and ADMIXTURE. The *ancient* dataset was used for outgroup *f*3 statistics, *f*4 statistics, Chromopainter/NNLS, *f*4 NNLS analysis and qpAdm.

Principal component analysis

Plink files were converted to EIGENSTRAT format using the program convertf from the EIGENSOFT 7.2.0 package with the parameter *familynames:NO*.[44,45] PCA was performed using the program smartpca with the parameter *autoshrink:YES*, projecting ancient individuals onto the components constructed based on the modern genotypes. The PCA was visualized using R-3.6.[87] The sampled individuals were projected on top of the present-day individuals in the David Reich dataset. A subset of ancient individuals from Eurasia were projected in groups (Figures 2A and S4; Data S1D).[4–7,9,10,12–15,23,24,46,47,64,65,114–121]

DyStruct

We modeled individuals as a mixture of different ancestral components by means of DyStruct, which takes into consideration temporal dynamics in the model based clustering method similar to admixture.[52] In detail, we performed five independent runs for K ancestral component K Î {2..10}, of 50 epochs each, using the same set of modern and ancient individuals used in PCA and ADMIXTURE analysis, and assigning them to time-interval of 1000 years, assuming generations of 25 years (Figures 2B and S2). To ease the visualization in Figure 2B, we focused only on Italian individuals together with a small subset of key Eurasian populations.

*f*4 statistics

For the *f*4 statistics, the same dataset as for the PCA was used and the target groups with 798 individuals from 191 ancient groups from Europe, Caucasus, Near East (Data S2). We performed *f*4 statistics in the form *f*4(Mbuti.DG, site1; site2, Y) for each studied site, whereby site 1 + 2 are the newly studied sites and Y is one of the comparative ancient groups/population (Data S2A). Additionally, we performed *f*4 statistics in form *f*4(Mbuti.DG, sample1; sample2, Y) as well as *f*4(Mbuti.DG, sample1; Y1, Y2) for each studied sample (Data S2C–S2F). We used ancient individuals from different context: Western Hunter-Gatherers, Eastern Hunter-Gatherers, Yamnaya Steppe/ Pontic Steppe, European Neolithic farmers, Anatolia Neolithic, and ancient Italian individuals from previously studies.[7,9,13,14,16,17] We used the program qpDstat with the option *f4mode:YES* from the software ADMIXTOOLS 4.1.[122]

Additionally, we performed *f*4 statistics in form *f*4(Mbuti.DG, Russia_EBA_Yamnaya_Kalmykia.SG/Samara, X, Anatolia_N) to test the affinity of all ancient Italian individuals spanning from the Neolithic to the Iron Age using qpDstats (Data S2B). The results of the

*f*4 statistics in form *f*4(Mbuti.DG, Russia_EBA_Yamnaya_Kalmykia.SG, X, Anatolia_N) were visualized using R 3.6[87] (See also Figures 2C and S4B).

Outgroup f3 statistics

For the study of X chromosome versus autosomes, outgroup $f3$ statistics in the form $f3$(Italian_CA/Italian_EBA_BA,X; Mbuti.DG) were performed with Mbuti.DG as the outgroup and the same subset of the ancient population previously described was chosen. For the analysis, the autosome and X chromosome positions available in Lazaridis et al.[46] ancient dataset were selected and the data was converted to EIGENSTRAT format using the program convertf from EIGENSOFT 7.2.0[44] with the parameter *familynames:NO*. To understand the sex-specific patterns detected in European Bronze Age populations, the newly generated samples were grouped according to the clusters seen in the PCA (Figure 2A) - Italy_CA (n = 12) and Italy_EBA_BA (n = 8). Published ancient individuals from Italian Peninsula were added to the groups following Italy_CA: Italy_C.SG (R1014.SG, R4.SG, R5.SG = 3),[13] Italy_North_Remedello_C.SG (RISE487.SG, RISE4879.SG = 2)[7] and Italy_EBA_BA: Italy_North_Remedello_EBA.SG (RISE486.SG = 1), Italy_North_Bell-Beaker (I1979, I2477, I2478 = 3).[9] Outgroup $f3$ statistics were computed using ADMIXTOOLS 1.1[122] option qp3Pop (See also Data S1K, Figure S5).

Additionally, we performed outgroup *f*3 statistics in form *f*3(Italy_CA, X; Mbuti.DG) to explore the genetic relationships of Italy_CA and peri-Neolithic groups (X) (Data S1K). The group Italy_CA contains following samples from the Italian Peninsula dated to the Chalcolithic: Italy_Broion_CA, Italy_Gattolino_CA, Italy_LaSassa_CA, Italy_C.SG, Italy_North_MN_Iceman_contam.S, and Italy_North_Remedello_C.SG.

Admixture analysis

We exploited the model-based algorithm implemented in ADMIXTURE[53] projecting ancient individuals (-P flag) into the genetic structure calculated on the modern dataset, due to missing data in the ancient samples. In detail, we performed unsupervised Admixture for K Î {2..10} for modern samples, and used the ''per-cluster'' inferred allele frequencies to project the ancient samples. We visualized the Q output using R 3.6[87] (Figure S3).

Chromopainter/NNLS and SourceFind

We reconstructed the ancestry of each individual using the Chromopainter (CP)/NNLS framework[55] and SourceFind (Figures 3 and S6). First, in order to obtain information from the highest number of markers, we painted all the Italian and a selection of European ancient individuals, using the unlinked mode, together with Loschbour_published.DG (Western European Hunter-Gatherer), I0061 (Eastern European Hunter-Gatherer), I0707 (Anatolia Neolithic), KK1.SG (Caucasus Hunter-Gatherer), HGDP00982 (Mbuti), I0443 (Yamnaya herders), against a set of 1,260 modern individuals (donors). We used 0.0002 and 318 as M and n parameters.[123] The resulting copying vectors, summarizing the number of markers inherited from each modern individual, were then pooled according to donors' affiliation and normalized to sum 1. Finally, we reconstructed each target individual copying vector as a mixture of different proportions of the putative surrogate sources, taking advantage of a slightly modified version of the nnls function in the ''nnls'' package in R software, and implemented in GlobeTrotter. In addition, in order to reduce the noise generated by the relatively low number of markers, the same analysis has been repeated using the putative source average copying vectors through all the ChromoPainter runs (Figure S6).

Additionally, the same analysis has been performed using SourceFind rather than the NNLS.[56,57] In detail, for each sample, we performed 10 runs of 5 million iterations thinned by 10,000 and discarding the first 50,000 iterations. The expected number of sources was set to 3 with a maximum of 4 possible sources. Only the iteration characterized by the highest Likelihood was shown in a barplot (Figure S6).

f4 NNLS analysis

In order to provide an additional description of ancestral composition of the analyzed samples we carried out a NNLS analysis using different $f4$ statistics vectors as a proxy of relations among different ancient groups. In detail, for any given target population, an $f4$ analysis in the form $f4$(X,Y, Target, Mbuti.DG) has been performed, where X, Y and target belong to one of 100 ancient groups from previously and newly genotyped data. In doing so, we obtain for each target a vector of 4,950 D Statistics; and we used the vectors for two different sets of putative sources to infer the ancestral proportions of a selection of European and Italian ancient samples, using the same nnls function of the Chromopainter/NNLS analysis (See also Figure S6). We used the following sets of sources:

Set 1: Luxembourg_Loschbour_published.DG, Anatolia_N, Iran_Tepe_Abdul_Hosein_N.SG, Russia_EHG
Set 2: Luxembourg_Loschbour_published.DG, Anatolia_N, Iran_Tepe_Abdul_Hosein_N.SG, Russia_Yamnaya_Kalmykia.SG

qpAdm

In order to describe the ancestry of Italian target individuals as a combination of prehistoric groups known to have played a major role in European demography, we harnessed the qpWave/qpAdm framework (Data S3). In details, for each sample, given a set of left and right populations, and for the number of left (sources) K Î {2..4} we:

a) Evaluated if the right samples can be used to significantly discriminate the provided sources, harnessing qpWave. Right populations present in sources were excluded for that specific test.
b) If step a) provided a significant p value < 0.01, we used qpWave to evaluate if the target sources could be described as a combination of K sources.
c) If b) provided a p value > 0.01, we used qpAdm to describe the target as a mixture of the K sources employed for that specific experiment. Given the high rate of missingness in some of our tested samples we used the option "allsnps=YES"

We used three different sets of left groups which we called "pre-Bronze Age," "post-Bronze Age," and "Continuity Neolithic"
pre-Bronze Age left panel:
Anatolia_N, Luxembourg_Loschbour_published.DG,Russia_EHG, Georgia_Kotias.SG
post-Bronze Age left panel:
Anatolia_N, Russia_Yamnaya_Samara, Luxembourg_Loschbour_published.DG
Continuity Neolithic left panel:
Russia_EBA_Yamnaya_Samara, Italy_Mesolithic.SG, Italy_C.SG, LaSassa, Broion_CA, Iberia_C, Germany_BellBeaker, France MN
In all cases we used the following right populations:
Russia_AfontovaGora3, Russia_EHG, Iberia_ElMiron, Belgium_GoyetQ116_1_published, Russia_Kostenki14, Jordan_PPNB, Russia_MA1_HG.SG, Israel_Raqefet_M_Natufian, Ust_Ishim.DG, Czech_Vestonice16, Georgia_Kotias.SG

Genome imputation

Following Hui et al.,[60] genotype likelihoods were first updated with BEAGLE 4.1[86] from genotype likelihoods produced by ATLAS[88] in Beagle -gl mode, followed by imputation in Beagle -gt mode with BEAGLE 5[124] from sites where the genotype probability (GP) of the most likely genotype reaches 0.99. To balance between imputation time and accuracy, we used 503 Europeans genomes in 1000 Genomes Project Phase 3[62] as the reference panel in Beagle -gl step, and 27,165 genomes (except for chromosome 1, where the sample size is reduced to 22,691 due to a processing issue in the release) from the Haplotype Reference Consortium (HRC)[72] in the Beagle -gt step. A second GP filter (MAX(GP) > = 0.99) was applied after imputation. Both new and published genomes were processed individually in the -gl step; in the -gt step, they were jointly imputed in the following groups:

All new genomes sequenced in this study; Mesolithic genomes (n = 3), Neolithic and Chalcolithic genomes (n = 13), Iron Age and later genomes (n = 11) from Antonio et al.;[13] Bronze Age Steppe: RISE509, RISE511, RISE547, RISE548, RISE550, RISE552 from Allentoft et al.;[7] EBA1 and EBA2 from Damgaard et al.;[65] Anatolia Neolithic: Bar31, Bar8, Klei10, Pal7, Rev5 from Hofmanová et al.;[5] WHG: KO1 from Gamba et al.;[125] Bichon from Jones et al.;[121] La Braña from Olalde et al.;[27] EHG: Sidelkino from Damgaard et al.;[65] CHG: KK1 and SATP from Jones et al.[121]

Runs of Homozygosity

We used hapROH[61] to detect runs of homozygosity (ROH) in ancient genomes. Using information from a reference panel, hapROH has been shown to work for genomes with more than 400K of the 1240K SNPs panel covered at an error rate lower than 3% in pseudo-haploid genotypes.[61] We note that the requirement is broadly in line with the imputation accuracy we get from coverages as low as 0.05x, where ~60% of common variants (MAF greater than or equal to 0.05) in the HRC panel are recovered with an accuracy greater than 0.95 in diploid genotypes.[60] Among common variants in the HRC panel, 853,159 overlap with the 1240K SNPs panel.

Nevertheless, imputation errors are not evenly distributed across the genome; the accuracy varies with the genotypes, minor allele frequency and local recombination rate, which may bias results in downstream analysis. We introduced random genotype errors into modern high-coverage genomes following the pattern observed in imputed ancient genomes. We then compare the total amount of ROH detected in the original genomes and the genomes with simulated imputation errors to explore whether hapROH can be used on imputed genomes.

Predicting imputation errors

A logistic regression model was developed to predict imputation errors from the features of the variant. Imputation accuracy has been shown to vary according to the true underlying genotypes (heterozygous sites have lower accuracy than homozygous sites) and minor allele frequencies (rarer variants have lower accuracy).[24,60,125] Since recombination breaks down linkage disequilibrium, the local recombination rate will also affect imputation accuracy via the number of linked sites. Finally we also included the substitution type (transition versus transversion) among the explanatory variables, because *post-mortem* damage in aDNA might be erroneously interpreted as C to T (or G to A) mutations. Considering that allele frequencies influence both imputation accuracy and ROH detection, a log-transformed MAF term was added in addition to the untransformed MAF to capture its effect more accurately. The recombination rate was also log-transformed. The header of Data S5 lists the explanatory variables and the transformation applied to each of them.

We down-sampled the 20x Neolithic Hungarian genome NE1 to 0.05x and ran it through the same imputation pipeline. The imputed genotypes were then compared to the confidently called genotypes in the original 20x genome to calculate the error rate. Because NE1 is older than all the genomes sequenced in this study, we expect to establish a lower bound of the performance of imputation from its result.

We fitted three separate multinomial logistic regression models to predict the imputed genotypes when the true genotype is homozygous for the reference allele (0/0), homozygous for the alt allele (1/1), or heterozygous (0/1). The outcome is a categorical variable with four values: missing genotypes (not passing the max(GP) greater than or equal to 0.99 post-imputation filter), 0/0, 0/1, and 1/1. Data S5A shows the coefficients and intercept for each model.

We then used the model to simulate the effect of imputation by introducing random genotype errors into a VCF file with high-quality genotypes. For each variant, we applied the softmax function on the scores for the four outcome categories (./., 0/0, 0/1, 1/1) to obtain the probability distribution before randomly drawing an "imputed" genotype. This allows us to quickly generate large numbers of "pseudo-imputed" genomes where the true genotypes are known for assessing the effect on downstream analysis without the lengthy process of down-sampling and imputation. Data S5B shows that the error pattern after imputation is well approximated by this approach when applied onto the original 20x NE1 genome.

Introducing imputation errors into modern genomes

We used the same model to introduce random error into 107 modern Italian (TSI) genomes from the 1000 Genomes Project Phase 3.[62] We extracted them from the HRC panel so that the list of variants is identical to what we get after imputation with HRC as the reference panel. We then used hapROH to detect ROH segments in both the original genomes and the genomes after introducing imputation errors. Except for switching from haploid to diploid mode, we kept the default parameters unchanged. We also used the default reference panel, 1000 Genomes Project data at 1240K sites, after masking out the TSI population. The relevant parameters to the hapsb_ind function are:

h5_path1000 g = 'all1240/chr', e_model = 'diploid_gt', p_model = 'EigenstratUnpacked', post_model = 'Standard', delete = False, n_ref = 2504, exclude_pops = ['TSI'], readcounts = True, random_allele = False, roh_in = 1, roh_out = 20, roh_jump = 300, e_rate = 0.01, e_rate_ref = 0.0, cutoff_post = 0.999, max_gap = 0, roh_min_l = 0.01

Figure S7A compares the total length (top) and number (bottom) of ROH tracks detected in the original genomes and the genomes with simulated imputation errors. In general the correlation is high for ROH segments longer than 1.6cM, although the total length is under-estimated in the presence of simulation errors when we filter for ROH segments longer than 4cM. This is most likely caused by longer ROH segments being broken down into shorter ones due to erroneous genotypes. Nevertheless outlier individuals with long ROH segments still stand out. The total number of ROH segments is reproduced less accurately in the simulated genomes than the total length of ROH segments.

In addition we tested a hidden Markov model-based ROH detection algorithm implemented in BCFtools[126] on the original and simulated genomes. Because this hidden Markov model-based algorithm takes allele frequencies in the population into account, we randomly divided the 107 individuals into 9 groups in order to 1) better match the sample size in this study and 2) reduce the running time of the analysis. Example command:

bcftools roh -G 30 -I -m genetic_map_chr{CHROM}_combined_b37.txt < input.vcf.gz > -o < output > -O r

Only ROH segments with a quality above 20 on the phred scale were retained. The result is similar to that from hapROH although the correlation is slightly lower (Figure S7B), supporting that the total length of ROH segments longer than 1.6cM can be reliably recovered in imputed genomes.

We also observed a strong correlation between the total ROH lengths detected by hapROH and BCFtools in the original genomes, which drops from ~0.97 to ~0.8 after imputation errors are introduced (Figure S7C). We chose to use hapROH on the ancient genomes out of two considerations. First, hapROH appears more robust in the presence of imputation errors (Figures S7A and S7B). Moreover, unlike BCFtools which processes a group of individuals together and utilizes allele frequencies in the population, hapROH examines one individual at a time. In this way it is less likely for our ROH result to be biased by the differences in sequencing coverage.

Detecting ROH segments in ancient genomes

We ran hapROH with the same setting as above on the imputed Chalcolithic and Bronze Age genomes generated in this study and the published Italian Mesolithic, Neolithic and Chalcolithic genomes (Data S1; Figure 4). For the 107 TSI genomes, we used results from the original genomes without the simulated errors.

Phenotype prediction

For the 41 HIrisPlex-S set of SNPs we selected 2 Mb around the informative variants, merging the regions on the same chromosome, with the exception of the variants on chromosome 15, which have been analyzed in two different regions since the distance between the two nearest SNPs was about 20 Mb. We finally selected 10 regions from 9 autosomes, spanning from about 1.5 Mb to 6 Mb. For the other phenotypic informative markers (diet, immunity and diseases), we selected 2 Mb around each variant and merged the overlapping region, for a total of 48 regions from 17 autosomes and X chromosome.

We called the variants using ATLAS v0.9.0[88] task = call and method = MLE commands at positions with a minimum allele frequency (MAF) greater than or equal to 0.1% in the reference panel, that has been selected according to the different components of the samples: 1) Europeans from 1000 Genomes (EUR),[62] for our Chalcolithic and Bronze Age Italians, for the pre-Imperial Romans from Antonio et al.[13] for pre-Nuragic and Nuragic Sardinians from Fernandes et al.[16] and Marcus et al.[17] and for Yamnaya;[4,7,64] 2) EUR plus the MANOLIS (EUR-MNL) set from Greece and Crete extracted from the Haplotype Reference Consortium (HRC)[72] (accessed at: http://www.haplotype-reference-consortium.org/) for the ancient Near Easterns, for non-Sardinian western Mediterraneans from

Fernandes et al.,[16] for post-Nuragic Sardinians from Marcus et al.[17] and for Imperial and Later Romans from Antonio et al.[13] (Table S4). After calling the variants separately for each sample, we merged them in one VCF file per region. We used the merged VCFs as input for the first step of our imputation pipeline[60] (genotype likelihood update), performed with Beagle 4.1 -gl command[86] using the same panels as before as reference. We then discarded the variants with a genotype probability (GP) less than 0.99 and imputed the missing genotype with the -gt command of Beagle 5.0[124] using the HRC as a reference panel for all groups of samples. We then discarded the variants with a GP < 0.99 and used the remaining SNPs to perform the phenotype prediction. Two markers of the HIrisPlex-S set, namely the rs312262906 indel and the rare (MAF = 0 in the HRC) rs201326893 SNP, were not analyzed because of the difficulties in the imputation of such variants. Results are reported in Data S6A–S6D.

We performed this analysis on our Chalcolithic and Bronze Age individuals and on published ancient samples from the Near East,[7,46,64,65] Italy[13,16,17] and Yamnaya population,[4,7,64] with a coverage greater than or equal to 0.05x. First, we grouped the individuals in six groups based on their location and time, namely two groups from Near East (Neolithic/Chalcolithic and Bronze Age), three from Italy (Neolithic/Chalcolithic, Bronze Age, post-Bronze Age) and one Yamnaya (Data S6A). We compared the groups performing an ANOVA test and, for the significant variants, we performed a Tukey test to identify the significantly different pairs of groups (Data S6B). We then analyzed the difference within Italy by creating 13 local groups (excluding 7 Sardinian individuals with an uncertain dating) (Data S6A) and comparing the 12 groups larger than 3 with an ANOVA test (Data S6C). For both comparisons, we used a Bonferroni's correction on an alpha value of 0.01 for the number of tested SNPs to set the significance threshold. We performed our phenotype analysis in a set of 332 ancient individuals, composed of the 16 Italian Bronze and Chalcolithic individuals reported here for the first time and 316 ancient Italians, Near Easterns and Yamnaya from the literature (Data S6A). Sample-by-sample phenotype prediction and genotype at the selected phenotype informative SNPs, reported as number of effective alleles (0, 1 or 2) are shown in Data S6D.